A New Synthesis of Testosterone[1].

By Yoshiyuki URUSHIBARA and Misao CHUMAN.

(Received October 1, 1948.)

The scission reactions of α- and β-cholesterol oxides and their acetates have been studied in this laboratory[2] since the configurations of these stereo-isomeric oxido compounds were inferred from known informations.[3] A configuration of 5,6-epoxy-cholestanol-(3β) (I) (α-oxido structure) was assigned to α-cholesterol oxide. Its acetate (I′) gave cholestane-diol-(3β,5α) 3-acetate (II′) on catalytic reduction. It was hydrolysed to the free diol (II), and oxidation to 5-hydroxy-cholestanone-(3) (III) followed by dehydration yielded Δ^4-cholestenone (IV).[2]

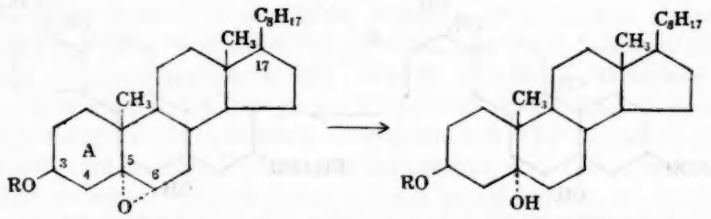

(I) R = H: α-Cholesterol oxide
(I′) R = CH_3CO: The acetate of I
(II) R = H: Cholestane-diol-(3β, 5α)
(II′) R = CH_3CO: The 3-acetate of II

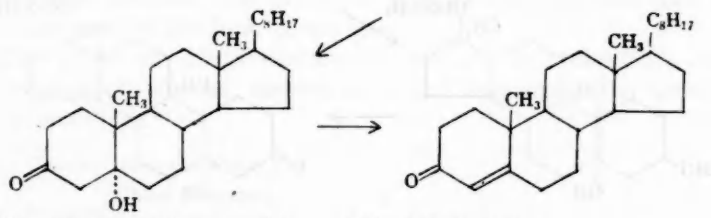

(III) 5-Hydroxy-cholestanone-(3)
(IV) Δ^4-Cholestenone

A similar course of reactions starting from α-dehydro-isoandrosterone oxide led successfully to a new synthesis of testosterone, a steroid hormone with ring A of the same structure as cholestenone. Two isomeric dehydro-isoandrosterone oxide acetates have been prepared, the higher melting isomeride (m. p. 221~222.5°) being designated as α and the lower melting (m. p. 188~190°) as β on the basis of the results of their acetolysis

(1) Abstract from the doctor thesis by M. Chuman. Read before the 68th annual meeting of the Chemical Society of Japan, on October 18th, 1946. Japanese Patent applied for on August 7th, 1946, and entered as No. 175210 on October 27th, 1947.
(2) M. Chuman, *J. Chem. Soc. Japan*, **64** (1943), 1369, 1486.
(3) Y. Urushibara, *this Bulletin*, **16** (1941), 182.

CHEMISTRY HALL LIBRARY

compared with those obtained with cholesterol oxide acetates[4]. Their configurations, however, had not yet been determined inasmuch as the designations α and β had been arbitrary in cholesterol oxides. α-Dehydro-isoandrosterone oxide acetate gave the changes corresponding to those of α-cholesterol oxide acetate, as described below, and thus was found to

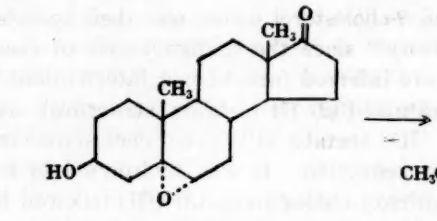

(V) α-Dehydro-isoandrosterone oxide (VI) The acetate of V

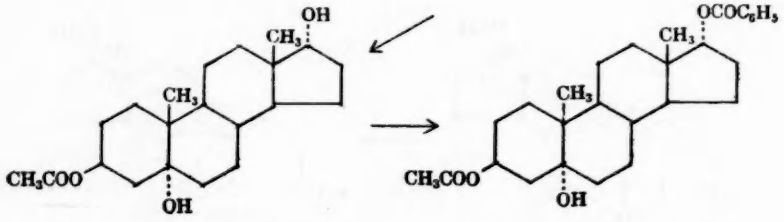

(VII) Androstane-triol-(3β, 5α, 17α) 3-acetate (VIII) The triol 3-acetate-17-benzoate

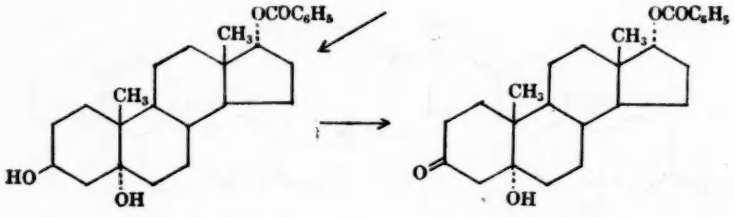

(IX) The triol 17-benzoate (X) 5α-Hydroxy-17α-benzoxy-androstanone-(3)

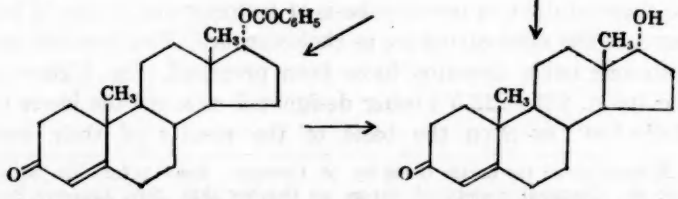

(XI) Testosterone benzoate (XII) Testosterone

(4) M. Ehrenstein, *J. Org. Chem.*, **6** (1941), 626. For earlier literature cf. *loc. cit.*

possess the same α-oxido structure (VI) as the latter, the configuration of which had been determined by one of the authors as mentioned above.

Catalytic reduction of α-dehydro-isoandrosterone oxide acetate (VI) (m. p. 220~221°), prepared from α-dehydro-isoandrosterone oxide (V) (m. p. 224~225°) with acetic anhydride and pyridine, with platinum oxide in glacial acetic acid gave androstane-triol-(3β,5α,17α) 3-acetate (VII), plates melting at 200~202° from acetone or ethyl acetate. On the reduction the oxido ring was splitted at the side of carbon atom 6 as in α-cholesterol oxide acetate[5] and the carbonyl group at carbon atom 17 was reduced to a hydroxyl group at the same time. The α- or trans-configuration of this hydroxyl group was determined because the triol finally gave (trans-)testosterone as described below.

The triol 3-acetate was benzoylated with benzoyl chloride and pyridine to androstane-triol-(3β,5α,17α) 3-acetate-17-benzoate (VIII), prisms melting at 232~234° from alcohol or ethyl acetate. Partial saponification with a calculated amount of methanol potash in two portions at the room temperature gave then androstane-triol-(3β,5α,17α) 17-benzoate (IX), flat needles or plates melting at 254~256° from acetone. Oxidation of the latter with chromic acid in glacial acetic acid at the room temperature yielded 5α-hydroxy-17α-benzoxy-androstanone-(3) (X), scales melting at 230~232° from alcohol, which was dehydrated with thionyl chloride and pyridine or better with hydrogen chloride in chloroform to testosterone benzoate (XI) melting at 180~182°. Saponification of the benzoate with methanol potash gave testosterone (XII) melting at 152~153°. The substance thus obtained was identified with an authentic specimen in the free state and in the form of acetate.

The action of dilute methanol potash on 5α-hydroxy-17α-benzoxy-androstanone-(3) effected saponification and dehydration to testosterone in one procedure.[6]

Chemical Institute, Faculty of Science,
Tokyo University

---

(5) By a similar catalytic reduction the oxido ring in β-cholesterol oxide acetate is splitted at the side of carbon atom 5 and cholestane-diol-(3β, 6β) 3-acetate (but none of coprostane derivatives) is formed.

(6) Japanese Patent applied for on March 20th, 1947. This improvement was not reported in the paper read before the annual meeting mentioned above but included in the doctor thesis by M. Chuman.

Ueber die intramolekularen Umlagerung des δ, δ-Diäthyl-γ-amino-δ-valerolactons.*

von Seizo KANAO.

(Eingegangen am 20. Mai 1945.)

Es wurde früher[1] vom Verfasser festgestellt, dass beim Grignardieren des α-Aminoglutarsäure-diäthylesters kein Aminoglykol wie beim Asparaginsäure-diäthylester[2] entstand, sondern unter Ringschluss [α-Pyrrolidonyl-(α′)]-dialkylcarbinol lieferte. Auf diese Weise erhielte Verfasser nicht nur Dialkyl-, Diaryl- bzw. Dialphyl-carbinol in der Pyrrolidonreihe, sondern auch die entsprechende in der Piperidonreihe aus dem α-Aminoadipinsäure-diäthylester Insbesondere stellt [α-Pyrrolidonyl-(α′)]-diäthylcarbinol (I) sehr schwach basische Prismen vom Schmp. 91–92° dar, die durch soda-alkalische 3, 5-Dinitrobenzoesäure kirschrot färben.

Durch Verseifen mit Barytlauge ging dieser Carbinol in eine δ,δ-Diäthyl-δ-oxy-γ-amino-*n*-valeriansäure (II) in fast quantitativer Ausbeute über, wobei sich solche Oxyaminosäure als prachtvolle Prismen vom Schmp. 143° abschied, die in wässriger Lösung die Polarisationsebene nach links, dagegen in salzsaurer Lösung nach rechts dreht. Sie wurde von ihrer β-Naphthalinsulfo-verbindung noch näher charakterisiert.

Leitete man trockenes Chlorwasserstoffgas in absolut alkoholischer Lösung der obigen Oxyaminosäure ein, so verwandelte sie unter Austritt von 1 Mol. Wasser in das δ,δ-Diäthyl-γ-amino-δ-valerolacton (III), das sich als krystallinisches Chlorhydrat vom Schmp. 209° gewonnen lies. Das freie Aminolacton stellt ein basisch riechendes Öl, $kp._{10}$ 126-127°, dar, welches bei Zimmertemperatur haltbar, aber in der Wärme nicht stabil ist; beim Vakuum-Erhitzen wandelte das Aminolacton grösstenteils in das erheblich hochsiedende Destillat ($kp._{13}$210-211°) um, das allmählich in sehr schwach basischen Krystallen erstarrte und die positive 3,5-Dinitrobenzoesäure-Reaktion gab; ausserdem erwies sich das letzte Umwandlungsprodukt in all den Eigenschaften mit dem [α-Pyrrolidonyl-(α′)]-diäthylcarbinol als identisch.

Auf Grund dieser Ergebnisse lässt sich daran bemerken, dass das Aminolacton durch Atomverschiebung eines in Aminogruppe vorhandenen Wasserstoffs nach benachbartem Lacton-Oxy in ein neues Lactam, nämlich Pyrrolidonderivat, übergegangen worden ist, und damit die genannte Umlagerung intramolekular stattfand. So ist die Beobachtung von E.

* Über die Umlagerung der Aminosäure u. ihrer Verwandten, VI. Mitteilung.

(1) *J. Pharm. Soc. Japan*, **48** (1928), 41; *Chem. Zentr*, 1928, II, 50.

(2) C. Paal u. E. Weidenkaff, *Ber.*, **39** (1906), 4344.

Fischer und H. Leuchs[3], ein Beispiel, dass das freie α-Amino-γ-valerolacton sich schon bei Zimmertemperatur unter Polymerisierung in Di-β-oxypropyl-diketopiperazin verwandelt; man könnte wenigstens daran denken, dass das δ,δ-Diäthyl-γ-amino-δ-valerolacton in freiem Zustande thermolabil ist.

Schliesslich möchte ich noch darauf hinweisen, dass die oben geschilderte Oxyaminosäure, die zuerst aus dem [α-Pyrrolidonyl-(α′)]-diäthylcarbinol geht, über Aminolacton unter ringschliessende Umlagerung in den [α-Pyrrolidonyl-(α′)]-diäthylcarbinol zurückkehrt, diese kreislaufende Umwandlung wohl als das folgende Schema aufzufassen ist:

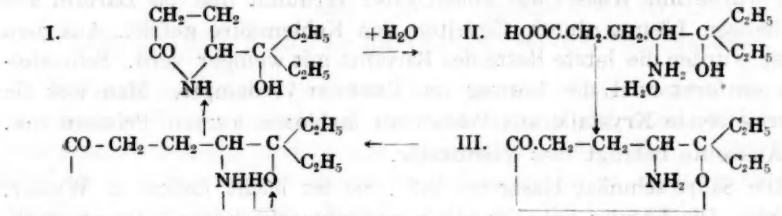

Beschreibung der Versuche.

[α-Pyrrolidonyl-(α′)]-diäthylcarbinol (I).

In einer Lösung aus 14.4 g. Magnesium, 65.7 g. Äthylbromid und mässigem absol. Äther wurden 20.3 g. *l* (+)-Glutaminsäure-diäthylester oder 15.7 g. *l* (−)-Pyrrolidoncarbonsäure-äthylester unter Kühlung allmählich zugegeben und auf den Wasserbade anderthalbe Stunde erwärmt. Das Reaktionsprodukt wurde mit Eis und berechneter Menge Phosphorsäure behandelt und Ammoniakwasser in die vom Äther abgetrennte sauren Lösung unter Erwärmen zugegeben. Die vom Ammoniummagnesiumphosphat abfiltrierte Lösung wurde im Vakuum eingeengt und ätzkalisch erschöpfend ausgeäthert. Der ätherische Auszug wurde über Natriumsulfat getrocknet und den Äther abdestilliert und der hinterbleibende Rückstand im Vakuum destilliert, wobei er fast alle unter 13 mm. bei 211° überging. Beim Umdestillieren gibt er kp.$_{7}$206°. Das zähe Destillat wurde dreimal aus Äther zu 9 bis 10 g. farblosen, langen Prismen krystallisiert. Der Körper schmilzt bei 91-92°.

Der spezif. Drehwert:

$$[\alpha]_D^{21} = -0.52 \times 18.4500/2 \times 1.0048 \times 0.6810 = -7.01 \text{ (in Wasser).}$$

Er löst sich leicht in Wasser, Alkohol, ziemlich in Äther, schwer in Petroläther. Aus der wässrigen Lösung scheidet er als Öl durch festem

(3) *Ber.*, **35** (1902), 3799.

Kaliumcarbonat aus. Beim Erwärmen mit 3,5-Dinitrobenzoesäure in Sodalösung färbt er kirschrot. Durch alkalische Kupferlösung (2% $CuSO_4$ u. 20% Natronlauge) zeigt er zuerst keine Veränderung, aber nach einiger Stunden schlägt er in purpur-blaue Farbe um, die von langsamer Ausbildung einer unten beschriebenen Oxyaminosäure verursachtet ist.

δ,δ-Diäthyl-δ-oxy-γ-amino-*n*-valeriansäure (II).

17.1 g. [α-Pyrrolidonyl-(α')]-diäthylcarbinol wurden mit 20%iger Barytlauge (40 g. Bariumhydroxyd) drei Stunden unter Rückfluss gekocht. Dann wurde mit Wasser auf einem Liter verdünnt und das Barium aus der heissen Lösung durch Einleiten von Kohlensäure gefällt. Aus dem Filtrat wurden die letzte Reste des Bariums mit weniger verd. Schwefelsäure entfernt und die Lösung im Vakuum verdampft. Man löst die hinterbleibende Krystalle aus Wasser zu farblosen kurzen Prismen um. Die Ausbeute beträgt fast quantitativ.

Die Säure schmilzt blasig bei 143°. Sie ist leicht löslich in Wasser, Alkohol. Die Lösung reagiert sauer und schmeckt bitter. Durch alkalische Kupferlösung gibt sie sofort purpurne Kupferverbindung, die in Wasser leicht löslich ist. Die Ninhydrin-Reaktion ist auch positiv.

$C_9H_{19}O_3N$ (189.16) Ber. N, 7.41. Gef. N, 7.53.

$[\alpha]_D^{20} = +3.36°$ (in Wasser); $[\alpha]_D^{20} = -14.48°$ (in 0.3 N-Salzsäure).[4]

β-Naphthalinsulfo-Verbindung der δ, δ-Diäthyl-δ-oxy-γ-amino-*n*-valeriansäure, $(C_2H_5)_2C(OH)-CH(NH\cdot SO_2\cdot C_{10}H_7)-CH_2-CH_2-COOH$.

Nach der Vorschrift von E. Fischer und P. Bergell[5] wurden 0.5 g. der Oxyaminosäure mit 10.5 c.c. N-Natronlauge (4 Mol.), 1 g. β-Naphthalinsulfochlorid in 15 c.c. Äther tüchtig geschüttelt, die von ätherische Schicht abgetrennte und filtrierte alkalische Lösung mit Salzsäure unter Kühlung angesäuert. Nach 3 stdg. Stehen in der Kälte wurden die Krystalle abgesaugt, die erst aus verd. Methanol und dann aus Methanol umgelöst wurden. Die Ausbeute beträgt annähernd quantitativ. Rhombische Prismen vom Schmp. 203° (unter Aufschäumen). In Alkohol, Aceton und heissem Methanol löslich. Die Verbindung ist langsam löslich in Kaliumbicarbonatlösung und gegen Lackmus schwach sauer.

$C_{19}H_{25}O_5NS$ (379.28) Ber. C, 60.11; H, 6.55; N, 3.69; S, 8.45.
Gef. C, 60.12; H, 6.81; N, 3.86; S, 8.19.

δ,δ-Diäthyl-γ-amino-δ-valerolacton (III).

(4) *J. Pharm. Soc. Japan*, **48** (1928), 357.
(5) *Ber.*, **35** (1902), 3779.

5 g. δ,δ-Diäthyl-δ-oxy-γ-amino-*n*-valeriansäure wurden in 30 c.c. absolutem Alkohol gelöst und durch Einleiten von trockenes Chlorwasserstoffgas gesättigt und darauffolgend auf dem Wasserbade eine halbe Stunde erwärmt. Dann wurde sie im Vakuum verdampft und der syrupösen Rückstand mit Äther über Nacht stehen gelassen, wobei es Krystallmasse lieferte, die man abfiltrierte und mit alkoholhaltigem Äther (1:9) nachwusch. Man löste sie aus Aceton-Äther zu weissen Nadeln um. Das Derivat schmilzt bei 209°. Es ist leicht löslich in Wasser, Alkohol. Die wässrige Lösung gibt durch alkalische Kupferlösung keine Farbreaktion, aber durch Ninhydrin zeigt sie eine rötliche Färbung.

$C_9H_{17}O_2N \cdot HCl$ (207.61) Ber. C, 52.02 ; H, 8.25 ; N, 6.74 ; Cl, 17.07.
Gef. C, 51.71 ; H, 8.46 ; N, 6.60 ; Cl, 17.27.

$[\alpha]_D^{22} = -0.05° \times 5.1403/1 \times 1.011 \times 0.1577 = -1.61°$ (in Wasser).

Freies Aminolacton : Das oben erwähnte Chlorhydrat wurde möglichst im geringen Wasser gelöst und unter Eiskühlung mit konz. Kaliumcarbonatlösung versetzt und öfters ausgeäthert, die über wasserfreies Natriumsulfat getrocknete ätherische Lösung möglichst rasch im Vakuum destilliert, wobei es unter 10 mm. Druck bei 126-127° siedete und die Hauptmenge in Pyrrolidonderivat verwandelt wurde.

Umlagerung von δ, δ-Diäthyl-γ-amino-δ-valerolacton.

Wurde diese Aminolacton langsam in Vakuum destilliert, so stieg die Temperatur auf und destillierte nach einiger stossartigen Erscheinung konstant unter 13 mm. Druck bei 210-211° aus. Das zähe Destillat wurde zweimal aus Äther zu Prismen krystallisiert, die den Schmp. 91-92° zeigten. Sie zeigten die 3,5-Dinitrobenzoesäure-Reaktion dagegen keine alkalische Kupferlösung-Reaktion mehr. Die Mischprobe mit dem oben erwähnten [α-Pyrrolidonyl-(α')]-diäthylcarbinol gab keine Depression. Der Analysen- sowie Dreh-wert stimmt auch mit dem Wert des letzten überein.

$C_9H_{17}O_2N$ (171.14) Ber. C, 63.10, H, 10.01 ; N 8.19.
Gef. C, 63.09, H, 10.06 ; N 8.28.

$[\alpha]_D^{20} = -0.47° \times 18.4476/2 \times 1.0042 \times 0.6077 = -7.10°$ (in Wasser).

Aus dem wissenschaftlichen Laboratorium von Dainippon-Kagakukogyokaisha (Gross-Japanisch Chem. Industrielle Aktiengesellschaft).

On the Configuration of Chain Molecules. II.

The effect of intramolecular interaction on the apparent volume of the flexible long-chain molecule.*

By Keizo SUZUKI.

(Received July 15, 1948.)

1. The standard state.

The configuration of the long chain molecule is a very important factor deciding the physical properties of its solution such as viscosity, diffusion, sedimentation velosity, etc.

If the parts of the chain have the tendency to bend irregularly, the long chain shows various configurations like the traces of a Brownian particle. The distance r of the both ends of such a molecule has the mean value

$$\langle r^2 \rangle = b^2 a^2 n \qquad (1)$$

where a is the length of an element of the chain, n is the number of the elements, and b is the constant showing flexibility. The value b^2 is 1 for the independently flexible elements, 2 for the free rotation model of paraffine, and about 6 for the hindered rotation model of it. The distribution probability of r is also known, but r expresses insufficiently the degree of 3-dimensional extension of the molecule. (Fig. 1).

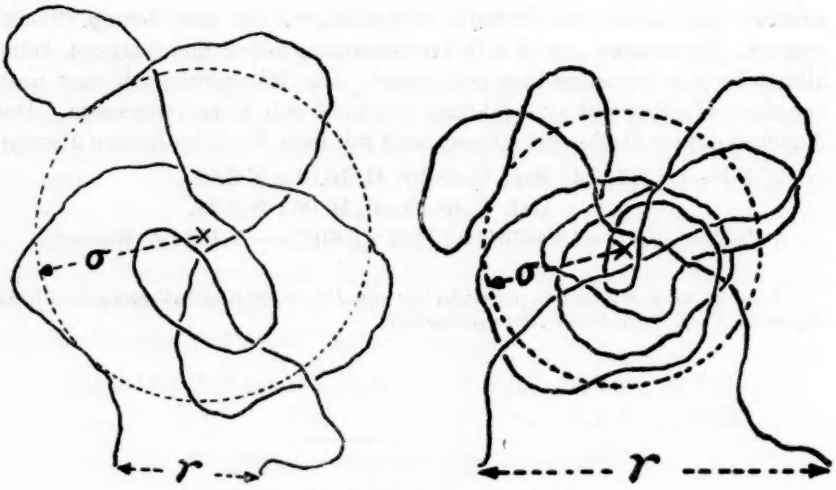

Fig. 1. The length r and the radius σ.

* Read in the annual meeting of the Society on Apr. 3, 1948.

Next, we take up 'the radius of gyration' for this purpose. Let $r_1, r_2, \ldots, r_i, \ldots$ be the distances of elements from the centre of mass, σ is defined by the formula

$$\sum r_i^2 = 3n\sigma^2 \qquad (2)$$

The mean square value of the radius of gyration of ordinary use around the axis through the centre of mass is equal to $2n\sigma^2$. σ_0, the square root of the mean value of the square of σ, for the molecule above shown, is given by the equation

$$\sigma_0^2 = \langle\sigma^2\rangle = \langle r^2\rangle/18^{(1)(2)} \qquad (3)$$

and the distribution of σ is in the similar type to that of r:

$$A\sigma^2 \exp(-\alpha\sigma^2)d\sigma, \text{ where } A = 4\sqrt{\alpha^3/\pi},\ \alpha = 3/2\sigma_0^2 = 27/b^2a^2n \qquad (4)$$

The state in which equations (1), (3) and (4) are correct is now named as the standard state.

2. The solvation energy.

These properties of the standard state have been derived on the assumption that there are no forces between the elements of the chain apart from each other on the chain. But however apart along the chain the elements near enough in the space can affect each other. If the energy of contact of the element is high, the molecule is apt to take the more extended configurations, and if low, the less extended. We shall discuss the effect of this energy on average values of σ, the quantity expressing the apparent volume of the molecule.

If the chain molecule is surrounded by other molecule of the same species, for example one of the isoprene polymers in rubber block, many of the elements of the chain may have no contact with any other elements of 'this' molecule, but must always be in contact with some other elements of 'other' molecules of the 'same' nature. Therefore the energy is independent of the contact of two parts of a molecule, and the ideal equations (1), (3) and (4) are correct. The condition is similar in the case where the surrounding molecules are separated into shorter chains. Thus we can say that there is no effect of the intramolecular attraction or repulsion in the solvents of the homologous series of the chain molecule, e. g. polyethylene in the solvents of paraffine series.

In other solvents the contacts are accompanied by some excess of energy, positive or negative. And the distribution is dominant in the

(1) K. Suzuki, this Bulletin, **20** (1947), 19.
(2) P. Debye, *J. Chem. Phys.*, **14** (1946), 636.

states of lower energy than those of higher energy, and the averages of σ will differ from those of the standard state.

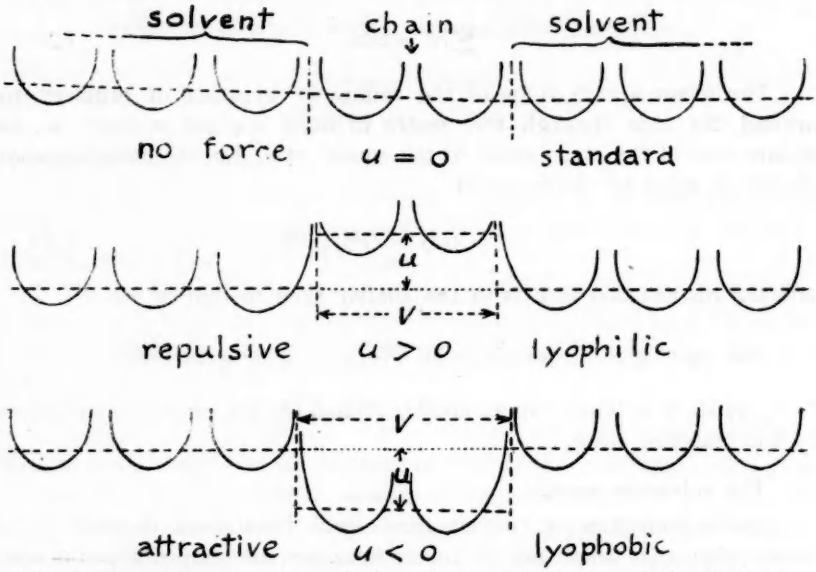

Fig. 2. Potential energy of an element of the chain in the neighbourhood of another element. u: contact energy. v: contact range.

The difference of energy due to the removal from the molecules of the same kind and the contact with solvent molecules is called 'solvation energy' and is the important factor which decides the apparent volume.

3. Contact number.

If an element is in the small volume v in the neighbourhood of another element, we consider that these elements are in contact with each other and have excess energy u compared with other two elements which are apart from each other and surrounded by solvent molecules.

The number of contacts f of this kind within a molecule must be given by the formula

$$f \propto vn^2\sigma^{-3}$$

This proportional constant is estimated as follows: the distribution probability of an element of a molecule of the given σ in the volume element $dxdydz$ in the Cartesian coordinate system with the origin at the centre of mass is

$$pdxdydz = (\sqrt{2\pi}\sigma)^{-3} \exp\{-(x^2+y^2+z^2)/2\sigma^2\}\, dxdydz \qquad (5)$$

The probability that another element is in the small volume v in the neighbourhood of the first is pv. The number of combinations of two elements is $n^2/2$. Then we can calculate the contact number by integration of the product of these three factors

$$f = \iiint p^2vn^2/2 \; dxdydz$$

and we get

$$f = vn^2\sigma^{-3}/16\pi^{1.5} \qquad (6)$$

The total excess energy U must be

$$U = fu = vun^2\sigma^{-3}/16\pi^{1.5} \qquad (7)$$

If there are various degrees of contact, and the values of energy are u_1 in the range v_1, u_2 in the range v_2, etc., then U must be

$$U = (v_1u_1+v_2u_2+\ldots.)n^2\sigma^{-3}/16\pi^{1.5} \qquad (7a)$$

The equation (7) includes the eq. (7a), if we consider that

$$vu = v_1u_1+v_2u_2+\ldots.$$

4. The corrected mean of σ .... approximation.

The distribution of σ must be corrected by the factor

$$\exp(-U/kT) \qquad (8)$$

But in the case where the change of this factor is not so large in the frequent range of σ, we can take only the first term of the expansion at the neighbourhood of $\sigma = \sigma_0$. Then we have

$$\langle\sigma^2\rangle = b^2a^2n/18+\sqrt{3}\,vun^{1.5}/4\pi bakT \qquad (9)$$

$$\langle\sigma^3\rangle = 4b^3a^3n^{1.5}/81\sqrt{3}+(15\pi-32)\,vun^2/64\pi^{2.5}kT \qquad (10)$$

The equation (9) giving the mean square of radius of gyration has the correction term proportional to $n^{1.5}$. This term is positive, when u is positive or in other words the solvation makes the energy low and the force between the parts of chain is repulsive. In the contrary this term is negative, when u is negative or in other words the solvation does not lower the energy and force is attractive. The behaviour of the second term of the equation (10) is quite similar.

It must be noticed that the ratio of the second term to the first term is proportional to $n^{0.5}$ and becomes larger with the increasing value of n. For it has been expected that the ratio of corrections of this kind tends to zero in the limiting case $n \to \infty$.

5. Specific viscosity....approximation.

If specific viscosity η_{sp} is given by Debye's formula

$$\eta_{sp}/c \propto \langle\sigma^2\rangle \tag{11}$$

where c is the weight concentration of the solution, eq. (9) leads to

$$\eta_{sp}/c = C_1 n + C_2 n^{1.5} \tag{12}$$

in which C_1 and C_2 are constants and their ratio must be

$$C_2/C_1 = 9\sqrt{3}\,vu/2\pi^2 b^3 a^3 kT = 0.788vu/b^3a^3kT \tag{12a}$$

If η_{sp} is given by Einstein's formula

$$\eta_{sp}/c \propto \langle\sigma^3\rangle/n \tag{13}$$

where $\langle\sigma^3\rangle$ is assumed to be proportional to the effective volume, then eq. (10) leads to

$$\eta_{sp}/c = C_1 n^{1.5} + C_2 n^2 \tag{14}$$

in which

$$C_2/C_1 = 81\sqrt{3}\,(15\pi\text{-}32)vu/16^2\pi^2 b^3 a^3 kT = 0.838vu/b^3a^3kT \tag{14a}$$

The value given by (12a) and (14a) contains no arbitrary constant. Now let us try a crude numerical estimation. In paraffine molecule the flexibility constant b^2 is about 6 according to the preceding paper. The contact energy u is assumed to be of the magnitude of the thermal energy kT. And the contact range v is probably about a^3, the volume of the cube with edges of the length of a C-C bond. Then C_2/C_1 in (12a) and (14a) is about 0.005, and the ratio of the second term to the first term in (12) or (14) becomes about $0.05n^{0.5}$. The correction amounts 50% even in the case where n is only 100. This result shows a cause of the failure of the formula of Staudinger's type

$$\eta_{sp}/c = \text{const. } n^{\alpha},\ \alpha = 0.5\sim1 \tag{15}$$

in applying over the wide range of n (Fig. 5).

This numerical value however seems to be somewhat contradictory to the assumption adopted in the approximation of eq. (8), that the correction is small. We must calculate more accurately.

6. Accurate formulae for repulsion.

Rewriting the factor (8) as

$$U/kT = \beta\sigma^{-3} \tag{16}$$

we calculate the numerical integrations

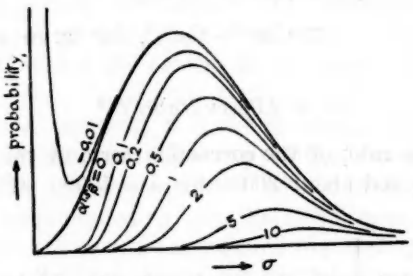

Fig. 3. The effect of intramolecular contacts on the distribution probability of σ.

$$\langle\sigma^2\rangle = \int\sigma^4 \exp(-\alpha\sigma^2)\exp(-\beta\sigma^{-3})d\sigma \Big/ \int\sigma^2\exp(-\alpha\sigma^2)\exp(-\beta\sigma^{-3})d\sigma$$
$$= 1.5\alpha^{-1}(1+f_2)$$
$$\langle\sigma^3\rangle = \int\sigma^5 \exp(-\alpha\sigma^2)\exp(-\beta\sigma^{-5})d\sigma \Big/ \int\sigma^2\exp(-\alpha\sigma^2)\exp(-\beta\sigma^{-3})d\sigma$$
$$= 4\pi^{-0.5}\alpha^{-1.5}(1+f_3)$$

and obtain the numerical values of f_2 and f_3 as the functions of $\alpha^{1.5}\beta$. (Fig. 4). They are proportional to $\alpha^{1.5}\beta$ when they are small, and proportional to the 0.4th and the 0.6th power of it respectively when they are large. Eqs. (4) and (16) give

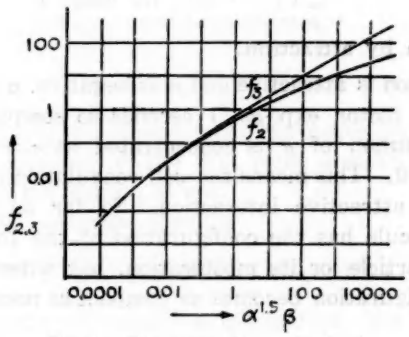

Fig. 4. The correction ratio f_2, f_3.

$$\alpha^{1.5}\beta = (27/b^2a^2n)^{1.5}vun^2/16^{1.5}kT$$
$$= 1.575vun^{0.5}/b^3a^3kT$$

Therefore f_2 and f_3 are proportional to $n^{0.5}$ for small n, and proportional to $n^{0.2}$ and $n^{0.3}$ respectively for large n (Fig. 4).

If the specific viscosity is given by Einstein's formula (13), we have

$$\eta_{sp}/c = \text{const.}n^{0.5}(1+f_3)$$
$$\cong C_1 n^{0.5} + C_2 n^{0.8}, \text{ for large } n \qquad (17)$$

where

$$C_2/C_1 = 2.08(vu/b^3a^3kT)^{0.6}$$

The numerical ratio of the correction term to the first term is about 70% for $n = 100$, and about 300% for $n = 10000$ (Fig. 5).

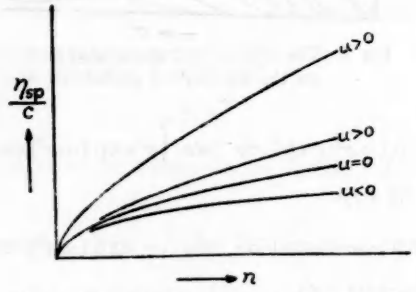

Fig. 5. The relation of viscosity to the molecular weight, and contact energy u.

We can obtain another formula from Debye's (11):

$$\eta_{sp}/c = \text{const.}n(1+f_2)$$
$$\cong C_1 n + C_2 n^{1.2}, \text{ for large } n \qquad (18)$$

7. Self-coagulation by attraction.

If the interaction is attractive and u is negative, β in eq. (16) becomes negative and the factor $\exp(-\beta\sigma^{-3})$ ascends so steeply when σ tends to 0 that the distribution of σ is concentrated at $\sigma = 0$. (Fig. 3). The averages of σ are 0. This means the self-coagulation of a chain molecule owing to its own attractive interaction. So far as the interaction is repulsive the molecule has the configuration of the form of the traces of a Brownian particle or its modification, but when the interaction is attractive the configuration becomes as compact as possible however small be the attraction.

Of course σ can not be just 0, because the smallest σ is that of the closest packed sphere of the molecule. But it may be regarded as 0 for large n in comparison with the loose extended form of the repulsive case. If we can alter the interaction gradually from repulsion to attraction by the change of the temperature or the change of the composition of the solvent,we must find the sudden contraction of the size

of the molecule at the moment when the solvation energy turns from positive to negative. It is similar to a phase change.

An example of the self-coagulation into the spherical form in bad solvent is given by the photograph of a polymer molecule by the electron microscope method, where the solvent is the worst one, the air or the vacuum.

If the number of elements n is not so large, the contraction may be gradual. For in this case the size of the closest packed sphere is not negligible so that the concentration of the distribution at $\sigma = 0$ is incomplete. The incompletion is not discussed here. But it is easily proved that we can obtain the approximation formulae (9), (10), (12) and (14) by cutting off the range of the false concentration into the spherical form of the distribution.

Summary.

In order to express the apparent size of a flexible long chain molecule the radius of gyration σ around the centre of mass is an appropriate quantity, and its mean square $\langle\sigma^2\rangle$ has been considered to be proportional to the number of elements of the chain n.

We estimate the effect of the intramolecular interaction and find new equations

$$\langle\sigma^2\rangle = \text{const.}n + \text{const.}n^{1.5}$$

$$\langle\sigma^3\rangle = \text{const.}n^{1.5} + \text{const.}n^2$$

Specific viscosity η_{sp} divided per weight concentration c must be

$$\eta_{sp}/c = \text{const.}n + \text{const.}n^{1.5}$$

or

$$\eta_{sp}/c = \text{const.}n^{0.5} + \text{const.}n$$

In these equations the second term can never be neglected for large n. It amounts to one half of the first term even in the case of normal paraffine with only 100 carbon atoms.

For large n the accurate formula

$$\eta_{sp}/c = \text{const.}n^{0.5} + \text{const.}n^{0.8}$$

is obtained in the case of repulsive interaction, but in respect to the molecule of large molecular weight with attractive interaction the self-coagulation into the very small size is concluded.

Masaoka-cho, Toyokawa, Aichi Pref., Japan.

The Quantum-Mechanical Treatment of Voscosity Coefficient of Helium by Use of a Rigid Sphere Model with Attractive Force.

By Kozo HIROTA.

(Received Sept. 1, 1948.)

1. Introduction.

In the former reports[1],[2], it was studied if the quantum-mechanical effect can fill up the gap between theoretical and experimental temperature dependency of the viscosity coefficient, and it was concluded definitely that the effect is short of explaining the gap in case of helium, so far as the rigid elastic sphere model is concerned. Therefore, the next step to be taken will be the introduction of molecular interaction in the calculation, as Massay and Buckingham[3] already did by use of Slater's potential. However, it was obliged to conclude that the concordance attained by them was limited in some narrow temperature-range, because the evaluation on higher temperatures was hindered by the cumbersome numerical integration. The final aim of the theory, therefore, has not been attained yet.

It is the object of the present paper to introduce a relatively less complicated model in the calculation, with the view to investigate the contribution of the molecular attraction on the collision phenomena. The well-known "Sutherland" model was adopted, assuming the potential form of inverse cube-law-force was the attractive potential to be utilized, i. e.,

$$V(r) = \infty, \quad \text{if } r < r_0 \quad \text{and} \quad \beta/r^2, \quad \text{if } r > r_0 \qquad (1)$$

where β denotes a constant and r_0 is the least distance of the molecular encounter.

The above attraction potential was adopted mainly for convenience's sake of the calculation, even though it is slightly improper as compared with the potential form of the sixth order, now aknowledged generally.

In the present report, the calculation was carried out on helium, keeping other assumptions as similarly as in the former report.[2]

II. Theoretical Formula.

(1) K. Hirota, A. Takahashi, and T. Yoshitomi, this Bulletin, **20** (1947), 1.

(2) K. Hirota, this Bulletin **19** (1944), 102.

(3) H. S. Massay and R. A. Buckingham, *Proc. Roy. Soc.*, A, **168** (1938), 304.

The aim of this paper can be reduced to a mathematical problem of evaluating the term (R) which is dependent on molecular interaction in Chapman-Enskog's formula[4] of the viscosity by use of such a model as (1):

$$\eta = \frac{10\kappa^2 T^3}{\mu}\left(\frac{4\pi\kappa T}{\mu}\right)^{\frac{3}{2}} \frac{1+\varepsilon_1+\varepsilon_2+\cdots}{\pi R} \tag{2}$$

where

$$R = \frac{1}{2}\int_0^\infty Q_\eta v^7 e^{-\frac{\mu v^2}{\kappa T}} dv \tag{3}$$

ε_ν: the ν-th order approximation term; Q_η: viscosity "Cross-section"; κ: Boltzmann's constant; μ and v: reduced mass and velocity of the colliding molecules, respectively; T: absolute temperature.

In the treatment, the first order approximation term (ε_1) was only calculated, while the higher order approximation terms (ε_2, ε_3, etc.) were neglected, according to the conclusion in the previous paper[1] that they are small irrespective to the model adopted.

The viscosity cross-section is given by[5]

$$Q_\eta = \frac{2\pi}{k}\sum_n \{1+\tilde{\varepsilon}^n\}\left\{\sin^2\delta_n \frac{4n^3-6n^2-2n+2}{(2n+1)(2n+3)}\right.$$
$$\left. -\cos(\delta_n-\delta_{n-2})\sin\delta_n\sin\delta_{n-2}\frac{2(n+1)(n+2)}{2n+3}\right\} \tag{4}$$

where $k = \frac{2\pi\mu v}{h}$ and $\tilde{\varepsilon}$ equals to 0, 1, -1 according as the statistics is Boltzmann's, Bose-Einstejn's or Fermi-Dirac's, respectively, and -1 was utilized throughout in this paper, because collisions of similar molecules were only dealt with. Summation was carried out with respect to all the scattered de Broglie's waves, and δ_n's are their phases which are to be determined from the solution of the wave equation with the boundary condition (1), i.e., the wave amplitude is zero at the molecular distance of r_0.

As the field is symmetrical to the centre of the scattering molecules, the problem is reduced to the solution of the radial part of the wave function u:

$$\frac{d^2u}{dr^2} + \left\{k^2 + \frac{n(n+1)}{r^2} - \frac{8\pi^2\mu}{h^2}V(r)\right\}u = 0 \tag{5}$$

---

(4) Chapman and Cowling, "Mathematical Theory of Non-Uniform Gases", Cambridge (1939).

(5) Cf. Chapman and Cowling, *ibid.*, Chapt. 17.

where r is the radial distance from the molecular centre of the colliding molecules.

Under the assumptions of (1),

$$\frac{d^2u}{dr^2}+\left\{k^2+\frac{n(n+1)-\gamma}{r^2}\right\}u=0 \qquad (5')$$

where $\gamma=8\pi\mu\beta/h^2$ at $r>r_0$ and 0 at $r<r_0$, the general solution is given by

$$U=\sqrt{r}\,\{AJ_{\nu_+}(kr)+BJ_{\nu_-}(kr_0)\} \qquad (6)$$

where ν_+ and ν_- denote $\nu_\pm=\frac{1}{2}(-1\pm\sqrt{(2n+1)^2+8})$, respectively.

The derivation of this formula is given by Mott and Massay.[6]

Taking the boundary condition $u=0$ at r_0 into consideration, we obtain

$$\delta_n=\operatorname{arctg}(-1)^n\{J_{\nu_+}(kr_0)/J_{\nu_-}(kr_0)\} \qquad (7)$$

where

$$v=(kh')/(2\pi\mu) \qquad (8)$$

III. Calculation and Results.

The numerical constants adopted in the calculation are as follows. The value of r_0 was assumed as 2.0 Å, because it was the best one in case of rigid elastic sphere models. The value of β was assummed as 8.9×10^{-32} c. g. s. and 1.12×10^{-32} for case A and B, respectively. They correspond to the assumption that the least energy at the distance of the molecular contact is, respectively, 800 and 1000 cal. Probably the least energy of attraction in the actual potential curve will exist within the two values. In other words, the attractive potential of liquid helium is estimated as such from the thermodynamic properties.

The procedure of calculation was perfectly similar to the case of rigid elastic sphere except the cumbersome evaluation of the Bessel function of non-integral orders. This most difficult procedure of the calculation was, however, simplified by the extrapolation of the values of Bessel functions $J_m(z)$ calculated by us.[7]

Thus it became possible to calculate the ratio of the quantal cross-section to that of the classical value (Q_n/Q_{n0}) in each two cases. The

(6) "Atomic Collisions". Oxford (1933), Chap. 1.

(7) Generally ν's in (6) become irrational numbers, so they are evaluated only when m equals to 0 0, $\pm$ 0.1, $\pm$ 0.2. $\pm$ 0.3, ..., $\pm$ 4.9, 5.0. It was found that values larger than $m=5$ were unnecessary in the present object.

results are shown by Table 1 together with that by use of a rigid elastic sphere model, as the function of kr_0. As is known the attractive potential made the effective collisional area larger, and the ratio is fairly near to that of a rigid elastic sphere model in case of small attractive potential (case B). It is also found that the larger the kr_0, the less is the effect, and in case of large attractive potential (case A), it is needless to calculate the values higher than $kr_0 > 10$, because they are practically equal to that of a rigid elastic sphere model.

By use of the values of case A, η was calculated according to (2), those of similar collisions being used. It was found that the effect of the attractive potential became marked at lower temperatures, and at 88.8°K the effect does not bring any change of figures (101.8×10^{-6}). However, it is clearly shown that introduction of such attractive potential contributes, to some extent, to fill up the gap hitherto found in case of rigid elastic sphere models. (cf. the last column of Table 2.)

Table 1. Effective "Cross-section" (Q_η/Q_{r_0}).

	Similar Collision			Dissimilar Collision		
kr_0	Rigid E. Sp. Model	Sutherland Model Case A.	Case B.	Rigid E. Sp. Model	Sutherland Model Case A.	Case B.
0.	8.000			4.000		
0.5	7.342			3.709		
1	5.535	6.673	5.63	3.108	3.64	3.18
1·5	3·585	3.727	—	2.556	2.500	—
2	2·287	2.163	2.271	2.168	2.217	2.17
2.5	1.866	1.895	—	1.653	1.973	—
3	1.757	1.960	1.795	1.780	2.075	1.809
4	1.596	1.638	1.599	1.570	1.642	1.598
5	1.466	1.448	1.462	1.468	1.498	1.464
7	1.327	1.332	—	1.329	1.345	—
10	1.234			1.229		
15	1.150			1.149		
20	1.113			1.110		
25	1.088			1.097		
30	1.070			1.070		
40	1.049			—		
50	1.039			—		

N. B. Case A. the least energy of attractive force 800 cal.
Case B. ..... 1000 cal.

On the other hand, it was found that larger values of β can make the η-values at 15°K smaller as much as we desire, though they cannot do so at 89°K at the same time. Such tendency can be amended, if

Table 2. Calculated and Experimental Values of Viscosity Coefficient of Helium.

T°K	Viscosity Obser.	Classical	Viscosity R. E. Sp.	calculated Model	Sutherland M.
		Value	$r_0=2.0$ A	$r_0=2.1$ A	$r_0=2.0$ A
1090	471.3	368	415.8	378.8	(415.8)
879	408.7	347	370.7	—	(370.7)
680	343.6	313	323.2	294.6	(323.2)
473	267.2	255	264.8	—	(264.8)
273.1	187.0	193	194.9	198.9	(194.9)
170.5	139.2	154	148.9	—	(148.9)
88.8	91.8	110	101.5	93.4	(101.8)
15.0	29.5	46	32.5	30.5	31.9

N. B. Values in parenthesis are the same as in the 4-th column.

we adopt a slower inclination of the repulsive potential. Thus we can got generally to a fairly good concordance of the theory and experiment, so far as monoatomic molecule is concerned.

Summary.

By use of a rigid sphere molecule model with attractive force of inverse cube law the viscosity coefficient of helium was calculated quantum-mechanically. It was found that the gap hitherto known between theory and experiment has become smaller at low temperatures than in case of no attractive force.

No. 70, 6-Chome, Siba-Shimbashi, Minato-ku, Tokyo.

Studies on Foams. II.

The Foam Formation and the Volume Contraction of Liquid Mixtures.

By Masayuki NAKAGAKI.

(Received Sept. 6, 1948.)

It has been reported, in the preceding paper,[1] that there are the maxima of the foam formation in three regions in the ternary system, ethyl alcohol-glycerol-water, that is the region of small concentration of ethyl alcohol, where the surface tension of the system decreases steeply, the region of large concentration of glycerol, where the viscosity of the system becomes very large, and the region of about 45 per cent of ethyl alcohol. The third maximum is thought to be closely connected with the volume contraction on admixture of the constituent liquids. This may be confirmed by the experiments, on the mixture of methyl alcohol, ethyl alcohol and water which is described in the following lines.

The experimental method is similar to that described in the preceding report. Foaminess and foam duration have been tested by shaking the liquid for 30 seconds in a test tube, measuring the height of foam zone immediately after the end of shaking (A_0 cm.), and the time required to the collapse of foam zone (t sec.). Viscosity η was measured with Ostwald's viscosimeter, and surface tension γ was measured with Traube's stalagmometer. Molar volume contraction ΔV on admixture of liquids (cc./mol.) was calculated from the density data obtained with an Ostwald's pycnometer.

The results obtained are shown in Fig. 1 and Fig. 2. The composition dependence of foaminess A_0 (Fig. 1), and foam duration t (Fig. 2), are entirely parallel with each other, having three maxima, A_1, A_2, and B_1. The maximum B_1 is, perhaps. related with the steep decrease of the surface tension, shown in Fig. 3. The maxima A_1 and A_2, on the other hand, have no relation either to surface tension or to viscosity (Fig 4). These

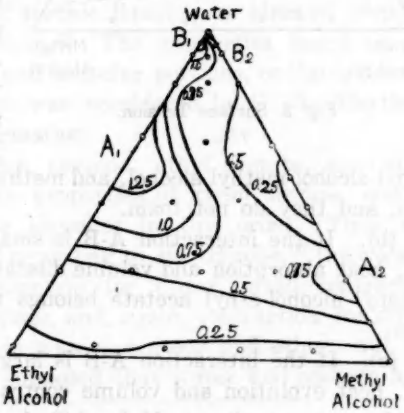

Fig. 1. Foaminess. A_0 (cm.).

(1) The first paper, this Bulletin, **21** (1948), 30.

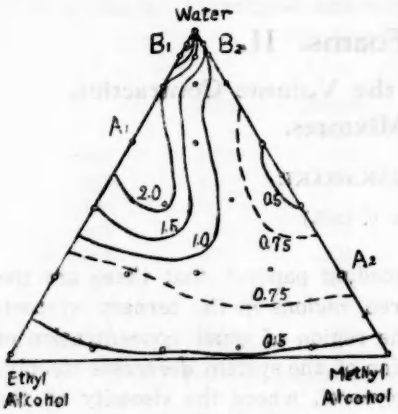

Fig. 2. Foam Durstion.
t (sec.).

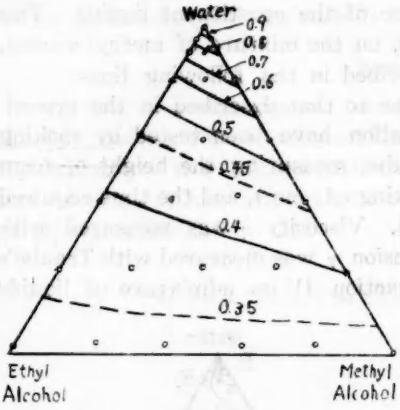

Fig. 3. Surface Tension.
τ/τ_w.

maxima seem to have some relation with the volume contraction (Fig. 5). Besides the ternary system, ethyl alcohol-methyl alcohol-water, the following five binary systems have been studied : *n*-propyl alcohol-ethyl ether, methyl alcohol-ethyl ether, ethyl acetate-ethyl ether, *n*-propyl alcohol-methyl alcohol and *n*-propyl alcohol-ethyl acetate. In most of these systems it was confirmed that the molar volume contraction is closely related to the foam formation. The system *n*-propyl alcohol-ethyl ether and methyl alcohol-ethyl ether have relatively large volume contraction and foam formation. The other systems have small volume contraction or dilatation and little tendency of foam formation.

The binary mixture of the liquid A and B may, generally, be classified into the following three types:

(a). If the molecular interaction between molecules A-B. is nearly equal to the average of A-A and B-B, heat of mixing and volume contraction on admixture are both small, and they forms the ideal solution. The systems *n*-propyl alcohol-methyl alcohol, and methyl alcohol-ethyl alcohol belong to this type, and they do not foam.

(b). If the interaction A-B is smaller than the average of A-A and B-B, heat absorption and volume dilatation may be observed. The system *n*-propyl alcohol-ethyl acetate belongs to this, and this system does not foam.

(c). If the interaction A-B is larger than the average of A-A and B-B, heat evolution and volume contraction on admixture are observed. In this case, according to McLeod,[2] viscosity-composition curve has a maximum point. Examples are the systems, ethyl alcohol-water and methyl

(2) McLeod, *Trans. Faraday Soc.*, **19** (1923), 17.

alcohol-water, the foam formation of which becomes maximum at the composition of about 1 : 1.

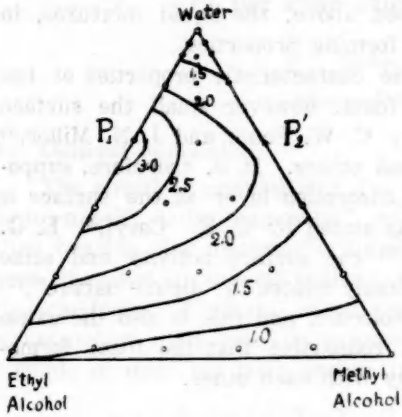

Fig. 4. Viscosity. η/η_w.

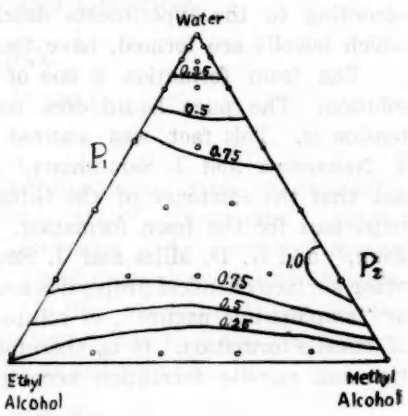

Fig. 5. Volume Contraction. ΔV (c.c./mol.).

Two mechanisms are proposed on the volume contraction. One is the increase of the average molecular interaction and the decrease of the average molecular distance, which may be corresponding to the case (c) described above. The other is the micelle formation of one of the constituent liquids. By the micelle formation the molecular motion will be restricted in some extent and the free volume of molecules may decrease. The idea that such a micelle is formed not only in aqueous solutions but also in the mixtures of organic liquids was already proposed by S. R. Palit and J. W. McBain.[3] The properties based on the simultaneous presence of the polar and nonpolar portions, or "amphipathic properties", of the solute molecule was considered by G. S. Hartley[4] as an essential factor of micelle formation.

Now a series of solvents, water, acetone, ethyl acetate, and ether will be considered. The hydrophile properties of them become weeker and the organic characters become stronger in this order. They mix with alcohol at any proportion, and according to H. Hirobe,[5] the volume change on admixture is large contraction for water, small contraction for acetone, dilatation for ethyl acetate, and, again, contraction for ether. Micelle may, probably, be formed in water, acetone and ether, but not in ethyl acetate. Therefore, it is supposed that water and acetone have

(3) S. R. Palit and J. W. McBain, *Ind. Eng. Chem.*, **38** (1946), 741.

(4) G. S. Hartley, "Aqueous Solutions of Paraffin-Chain Salts", London (1936), Chap. 7.

(5) H. Hirobe, *J. Faculty of Sci. Imp. Univ. Tokyo*, Sec. 1, **1**, Part 4 (1926), 155.

a stronger affinity for hydroxyl group of alcohol than for alkyl group, but ethyl acetate has nearly equal affinity for both groups, and ether has a stronger affinity for alkyl group than for hydroxyl group. Then, according to the experiments described above, the liquid mixtures, in which micelle are formed, have foam forming properties.

The foam formation is one of the characteristic properties of the solution. The pure liquid does not foam, however small the surface tension is. This fact was assured by C. W. Foulk and J. N. Miller,[6] T. Nakagawa and J. Sameshima,[7] and others. It is, therefore, supposed that the existence of the Gibbs' adsorption layer at the surface is important for the foam formation. As stated by C. R. Caryl,[8] E. G. King,[9] and G. D. Miles and J. Ross,[10] the surface activity and some other surface chemical properties are closely related to "diphile nature",[11] or "amphipathic nature", of solute molecule, and this is also the cause of micelle formation. It is, therefore, reasonable that the foam formation and micelle formation accompany with each other.

Summary.

The foam formations were tested on the ternary system, methyl alcohol-ethyl alcohol-water, and five binary mixtures. It was found that the volume contraction is closely connected with the foaming properties. This was interpreted in relation to the micelle formation of mixtures.

The author wishes to express his hearty thanks to Professor J. Sameshima for his kind guidance and encouragement.

Chemical Institute, Faculty of Science,
Tokyo. University

(6) C. W. Foulk, *Ind. Eng. Chem.*, **21** (1929), 815; **33** (1941), 1086; C. W. Foulk and J. N. Miller, *ibid.*, **23** (1931), 1283.
(7) T. Nakagawa and J. Sameshima, *J. Chem. Soc. Japan*, **64** (1943), 360.
(8) C. R. Caryl, *Ind. Eng. Chem.*, **33** (1941), 731.
(9) E. G. King, *J. Phys. Chem.*, **48** (1944), 141.
(10) G. D. Miles and J. Ross, *J. Phys. Chem.*, **48** (1944), 280.
(11) Wo. Ostwald, *Kolloid-Z.*, **58** (1932), 179; **60** (1932), 324.

General Expressions of the Chemical Compositions of the Fine Micas and Chlorites.

Toshio SUDÔ.

(Received July 15, 1948.)

1. General expression

The chemical compositions of so-called fine micas, such as sericite[1], hydro-mica[2], hydro-muscovite[3], secondary mica[4], glimmerton[5], potassium bearing clay minerals[6], illite[7], glauconite and celadonite[8], have been discussed by several authors, but these discussions had no basis on the standpoint of crystal structures. On the other hand, the crystal structure of mica, such as muscovite, was determined and the general formula of mica has been shown to be as follows[9]:

$$X_{0-1}Y_{2-3}(Z_4O_{10})(OH,F)_2$$

(Where X : K, Na, Ca ; Y : Al, Fe‴, Fe″, Mg, Mn, Cr, Ti, Li, V, etc. ; Z : Si, Al)

This formula has not been adapted to the chemical compositions of the fine micas above enumerated. The writer re-examined the chemical compositions of the fine micas by the general structural formula of mica, that is, the writer summarized the accurate and already reported chemical compositions of fine micas (Table 1. 2), and from these, the writer calculated X, Y, and Z of the formula above described, and values of X, Y, and Z thus calculated were plotted on the triangular diagram as shown in Fig. 1, (a), and (b).

(1) E. V. Shannon, *U. S. Natl. Museum Bull.*, **131** (1926), 367 ; J. Jakob, C. Friedlaender and E. Brandenberger, *Schweiz, Mineralog. u. Petrog. Mitt.*, **13** (1933), 74 ; P. Niggli, *ibid.* **13** (1933), 84 ; J. Jakob, *Z. Krist.*, **69** (1929), 511 ; B. Kotō, *J. Coll. Sci. Imp. Univ. Tokyo*, **2** (1888), 89.

(2) W. S. Bradley, *Econ. Geol.*, **15** (1920), 236 ; R. E. Somer, *J. Wash. Acad. Sci.*, **9** (1916), 113 ; A. Brammall, *Mineralog. Mag.*, **24** (1937), 507.

(3) G. Nagelschmidt, *Z. Krist.*, **97** (1937), 514.

(4) G. M. Schwartz and R. J. Leonard, *Am. J. Sci.*, **11** (1926), 262.

(5) K. Fndell, U. Hofmann, and E. Maegdefrau, *Zement*, **24** (1935), 625.

(6) C. S. Ross and P. E. Kerr, *J. Sed. Petr.*, **1** (1913), 59.

(7) R. E. Grim, R. H. Bray and W. F. Bradley, *Am. Mineral.*, **22** (1937), 813.

(8) Recently it has been shown that the types of glauconite and celadonite are similar in their X-ray powder patterns to those of micas. J. W. Gruner, *Am. Mineral.*, **20** (1935), 699 ; E. Maegdefrau and U. Hofmann, *Z. Krist.*, **97** (1937), 514.

(9) Ch. Mauguin, *Comp. rend. Acad. Sci. Paris*, **185** (1927), 288 ; **186** (1928), 879, 1131 ; L. Pauling, *Proc. Nat. Acad. Sci. U. S. A.*, **16** (1930), 123 ; W. W. Jackson and J. West, *Z. Krist.*, **76** (1931), 211 ; W. L. Bragg, "Atomic Structure of Minerals," 1937, 213.

Table I. (Sericite).

	(1)	(2)***	(3)***	(4)	(5)	(6)
SiO_2	46.58	50.39	50.05	45.64	47.14	53.01
TiO_2	.....	0.42	0.14	1.81	.....	.....
Al_2O_3	37.46	29.74	30.11	33.59	37.13	34.70
Fe_2O_3	0.80	1.61	1.47	1.96	0.64	tr.
Cr_2O_3	.....	.....	.....	.....	.....	.....
FeO	.....	0.38	0.43	0.38	.....	.....
MnO	.....	0.01	0.01	0.10	.....	.....
CaO	tr.	0.00	0.00	0.00	0.71	0.27
MgO	1.16	2.40	2.49	2.33	0.17	0.50
Na_2O	0.64	2.62	1.97	1.59	0.65	1.01
K_2O	6.38	9.97	9.80	8.81	9.98	6.05
$H_2O(+)$	6.06	2.55	3.58	3.89⊗	4.28*	4.67**
$H_2O(-)$	0.30	.....	.....	0.00⊕		
F	.....	.....	.....	.....	.....	.....
Total	99.38	100.09	100.05	100.10	100.70	100.21

Note: * Ig. loss. ** H_2O. *** analyses on material dried at 110°C.
⊗ > 110°C. ⊕ < 110°C.

(1) The Carrol-Driscoll Mine, Idaho. E. V. Shannon, *U. S. Natl. Museum, Bull.*, **131** (1926), 367.

(2) Werkkanals des Rheinkraftwerks, Albdruck-Dogern. Occurs in gneiss. Coarse grains accumulated by water dressing. J. Jakob, C. Friedlaender and E. Brandenberger: *Schweiz. Mineralog. u. Petrog. Mitt.*, **13** (1933), 74; P. Niggli: *Schweiz. Mineralog. u. Petrog. Mitt.*, **13** (1933), 84.

(3) As (2), fine grains.

(4) Campra bei Olivone, Kanton Tessin. Fine scales in sericite biotite schist, forming nests partly. J. Jakob: *Z. Krist.*, **69** (1929), 511.

(5) The Hitachi Mine, Ibaragi Prefecture. K. Seto: *J. Japan. Assoc. Mineral. Petrol. Econ. Geol.*, **1**. (1929), 124.

(6) Ōtakisan in Tokushima Prefecture. B. Kotō: *J. Coll. Sci. Imp. Univ. Tōkyō*, **2** (1888), 89.

From these figures the following general facts are recognized:

(1) The plotting points of the colourless fine micas such as sericite, hydro-mica, secondary mica, illite, etc., and the plotting points of the chemical compositions of glauconite and celadonite fall in the same area. (Fig. 1, (a), (b)).

(2) The fine micas have, as a rule, less X(K, Na, Ca) and more Y(Al, Fe‴, Fe″, Mg, etc.) than muscovite (M), and such fluctuation is largest in illite. (Fig.1, (a)).

(3) From Fig. 1 (b) the differences in the chemical compositions of glauconite and celadonite are not clearly shown.

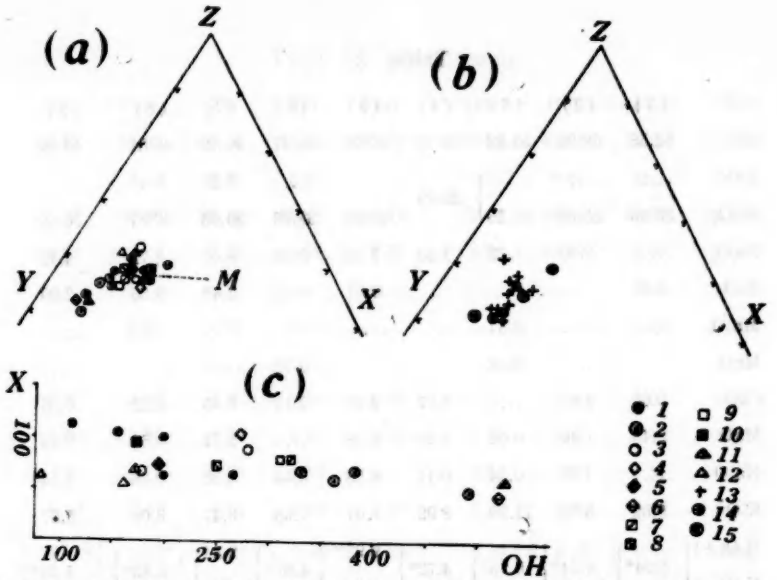

Fig. 1. 1, Sericite; 2, Illite; 3, Phengite; 4, Alurgite; 5, White mariposite; 6, Hydro-mica; 7, Hydro-muscovite; 8, Secondary muscovite; 9, Damourite; 10, Gilbertite; 11, Micas altered from spodumene; 12, Micas reported by E. Maegdefrau and U. Hofmann; 13, Glauconite; 14, Celadonite; 15, "Grünerde" (by K. Hummél); *M*: Mean value of the chemical compositions of muscovite (by W. Kunitz, *Neues Jahrb. Mineral. Geol.*, Beilage-Band, A, **50** (1924), 365.)

2. Relation between (OH) and (K, Na, Ca) of the fine micas.

Next the writer compared the content of (OH)[10] and that of X(K, Na, Ca) as shown in Fig. (1), (c). It is shown, from Fig. 1, (c), that the content of (OH) is roughly inversely proportional to the content of X(K, Na, Ca). The writer also compared the ratio of SiO_2/Al_2O_3 and the content of X(K, Na, Ca), but no fixed ratio has been found between these values.

In the chemical compositions of glauconite and celadonite, we could not recognize the fixed ratio between the values of (OH) and X(K, Na, Ca), or (OH) and the ratio of SiO_2/Al_2O_3.

3. R_2O_3/RO in glauconite and celadonite.

In Fig. 1, (a) and (b), the differences between the chemical compositions

(10) It is a very difficult problem to solve the state of the water in the crystal structures of such fine micas. In the chemical analyses reported in literatures, the water contents are described in various forms, such as $H_2O(+)$ and $H_2O(-)$ or only as H_2O or as ignition loss. Generally the content of $H_2O(-)$ is small, and the writer used the value of $H_2O(+)$ when the content of water is described separately as $H_2O(+)$ and $H_2O(-)$, and in other cases, he used the total content of water or ignition loss.

Table 2.

	(1)	(2)	(3)	(4)	(5)	(6)	(7)	(8)	(9)
SiO_2	52.58	58.90	53.22	56.79	47.29	53.47	40.79	46.54	46.54
TiO_2	.....	.....	.....	25.29	.....	.....	1.28	0.17	.....
Al_2O_3	23.56	25.28	21.19		31.31	32.36	29.98	36.37	30.39
Fe_2O_3	.....	2.30	1.22	1.59	1.19	0.79	8.07	0.72	4.42
FeO	5.76	.....	.....	....	0.37	0.42	2.48	0.36	2.98
Mn_2O_3	.....	.....	0.87	.....	.....	.....	.....	.....	.....
MnO	.....	.....	0.18	.....	.....	0.72	.....	.....	.....
CaO	0.65	0.65	.....	0.07	0.69	0.17	0.45	0.22	0.35
MgO	2.43	1.49	6.02	3.29	2.38	.....	2.71	0.50	0.94
Na_2O	.....	1.37	0.34	0.17	0.88	0.44	0.38	0.46	1.44
K_2O	9.52	5.73	11.20	8.92	4.07	7.68	3.47	8.06	5.57
$H_2O(+)$	5.94*	4.14*	5.75*	4.72*	9.92**	4.07*	9.34	6.83*	5.31**
$H_2O(-)$					1.88		1.20		
F	.....	.....	.....	.....	.....	.....	.....	0.02	0.58
Total	100.44	99.86	99.99	100.84	(100.26)	(100.16)	(100.15)	100.25	98.52

Note: *H_2O; **Ig. loss; †Ig. loss on material dried at 110°C; ††Ig. loss on material

(1) Phengite (Wildschapbachtal). "Doelter's Handbuch der Mineralchemie", II, Part 2 (1917), 428.

(2) Phengite (Witticher Tal). "Doelter's Handbuch der Mineralchemie", II, Part 2 (1917), 428.

(3) Alurgite (A manganese mine at St. Marcel, Piemont, Italy). S. L. Penfield, *Z. Krist.*, **25** (1896), 277.

(4) White mariposite (The Josephine Mine, Bear Valley, California). W. L. Hillebrand, *U. S. Geol. Survey Bull.*, **167** (1900), 74. Cr_2O_3: none.

(5) A micaceous mineral altered from spodumene (The Etta mine, South Dakota), G. M. Schwarz and R. J. Leonard, *Am. J. Aci.*, **11** (1926), 262. Li_2O: 0.28.

(6) A micaceous mineral altered from spodmene (Branchville, Connecticut). G. J. Brush and E. S. Dana, *Z. Krist.*, **5** (1881), 210. Li_2O: 0.04.

(7) Hydro-mica (North Carolina). W. S. Bailey, *Econ. Geol.*, **15** (1920), 236.

(8) Hydro-muscovite. G. Nagelschmidt, *Z. Krist.*, **97** (1937), 514. Li_2O: tr.

(9) Secondary muscovite (Spprechstein). "Doelter's Handbuch der Mineralchemie", II, Part 2 (1917), 426.

Table 2. (Continued).

(10)	(11)	(12)	(13)	(14)	(15)	(16)	(17)⊕	(18)⊕
45.72	48.96	50.10	51.22	47.21	52.23	44.01	51.65	50.30
.....	.....	0.50	0.53	.....	0.37	0.64	tr.	tr.
37.17	30.96	25.12	25.91	21.47	25.85	26.81	21.67	32.80
2.18	.....	5.12	4.59	10.73	4.04	11.99	6.20	0.00
.....	.....	.....	.....	.....	.....	.....	.....	.....
.....	2.24	1.52	1.70	.....	.....	.....	1.24	0.00
.....	.....	.....	.....	.....	.....	.....	.....	.....
0.05	0.26	0.35	0.16	0.21	0.60	0.11	0.00	0.55
2.00	1.97	3.93	2.84	3.62	2.69	2.43	4.48	1.95
1.44	1.65	0.05	0.17	.....	0.33	0.07	0.31	0.52
6.69	8.47	6.93	6.09	5.78	6.56	4.78	6.08	6.72
6.79*	3.83*	6.82†	7.49†	10.99††	7.88†	9.19†	6.44	6.98
....	1.04	....	....	....	....	....	....	....
102.04	99.38	100.44	100.70	100.01	100.55	100.03	98.07	99.82

dried in air; ⊕Chemical; analysis is of 105°C dried material.

(10) Damourite (Fen Norway). "Doelter's Handbuch der Mineralchemie", II, Part 2 (1917), 422.

(11) Gilbertite (Ehrenfriedersdorf). "Dana's System of Mineralogy", 1914, 618.

(12) Illite (Maquoketa (Ordovician) shale, near Gilead, Calhoun County, Illinois). $H_2O(+)$: 7.18; $H_2O(-)$: 1.90. R. E. Grim, R. H. Bray and W. F. Bradley, *Am. Mineral.*, **22** (1937), 813.

(13) Illite (Pennsylvanian underclay, near Fithian, Vermilion County, Illinois). $H_2O(+)$: 7,14; $H_2O(-)$: 1.45. Ref. as (12).

(14) Illite (IV b horizon of Clarence soil, Ford County, Illinois). $H_2O(+)$: 6.17; $H_2O(-)$: 3.80. Ref. as (12).

(15) Illite (Cretaceous shale, near Theles, Alexander County, Illinois). $H_2O(+)$: 7.88; $H_2O(-)$: 1.13. Ref. as (12).

(16) Illite (Pennsylvanian shale, near Petersburg, Menard County, Illinois). $H_2O(+)$: 8.03; $H_2O(-)$: 2.33. Ref. as (12).

(17) Mica in marl. Small amount of quartz is included in the analysed sample. E. Maegdefrau and U. Hofmann, *Z. Krist.*, **98** (1938), 31.

(18) Mica in liparite. Sarospatak, North-east of Mt. Hegyalja. Ref. as (17).

Table 3.

	(1)	(2)	(3)	(4)	(5)	(6)	(7)	(8)	(9)
SiO_2	51.55	51.38	51.63	51.25	50.75	51.27	53.58	48.66	48.5
TiO_2	tr.	tr.	tr.	tr.	tr.	tr.	0.07	.....	....
Al_2O_3	4.03	4.25	5.01	4.44	6.65	5.45	8.17	8.46	9.0
Fe_2O_3	22.17	23.82	23.09	22.22	21.64	23.14	18.27	18.80	20.0
FeO	3.54	2.91	2.75	3.62	3.41	2.85	2.87	3.98	3.1
MnO	tr.	tr.	tr.	tr.	tr.	tr.	tr.	.....	....
MgO	3.86	3.23	3.71	3.53	3.23	3.97	2.95	3.56	3.7
CaO	0,69	0.55	0.35	0.62	0.57	0.49	0.89	0.62	0.4
Na_2O	0.55	0.78	0.68	0.94	0.75	0.28	0.94	none	1.5
K_2O	7.03	6.82	6.75	6.95	6.92	6.80	5.64	8.31	6.2
P_2O_5	0.03	tr.	0.02	tr.	tr.	tr.	tr.	.....	....
CO_2	.....	.....	.....	.....	.....	.....	.....	.....	....
$H_2O(+)$ $H_2O(-)$	6.62*	6.62*	6.25*	6.23*	6.02*	6.00*	6.53*	4.62 1.94	7.3**
Total	100.07	100.36	100.24	99.80	99.94	100.25	99.91	98.95	99.67

Note: *H_2O; **Ig. loss; *** chemical analysis of 105°C dried materials;

(1)-(7) Glauconite from Japan (after T. Yagi) "Glauconite" (in Japanese).
(8) Glauconite. J. W. Gruner, *Am. Mineral.*, **20** (1935), 699; with CO_2, total 99.08.
(9) Glauconite. H. Schneider, *J. Geol.*, **35** (1927), 296.

Table 3. (Continued).

(10)	(11)	(12)***	(13)	(14)	(15)***	(16)	(17)	(18)	(19)
48.12	49.42	49.10	53.61	49.11	55.30	54.30	54.84	54.22	46.65
.....	.....	nb.	.....	.....	nb.	tr.	.....	.....	0.73
9.16	10.23	19.30	9.56	8.03	10.90	5.08	3.52	3.70	17.92
19.10	16.01	7.52	21.46	20.05	6.95	14.77	12.64	12.50	10.09
3.47	3.00	2.87	1.58	3.05	3.54	4.82	4.90	4.75	4.25
.....	.....	.....	tr.	.....	.....	0.09	0.24	0.19	0.07
2.36	3.78	2.71	2.87	3.18	6.56	6.05	6.65	6.98	1.63
0.76	0.31	0.98	1.39	0.87	0.47	0.80	0.89	0.84	1.26
0.22	0.26	0.00	0.42	0.66	0.00	3.82	0.39	0.44	0.69
7.08	7.91	7.50	3.49	6.97	9.38	4.85	7.00	6.90	3.91
.....	.....	.....	.....	.....	.....	.....	.....	.....	0.04
.....	.....	.....	.....	.....	.....	.....	.....	.....	1.66
5.28⊗	8.08*	6.07	5.96*	8.05*	5.21	5.64*	9.62*	99.9*	5.07
4.78⊕		....			....				5.86
100.33	99.00	96.05	100.34	99.97	98.31	100.22	100.69	100.51	99.83

⊗ > 105°C; ⊕ < 105°C.

(10) Glauconite. A. F. Hallimond, *Mineralog. Mag.*, **19** (1922), 330.

(11) As (10); quartz: 0.80%.

(12) Glauconite. E. Maegdefrau and U. Hofmann, *Z. Krist.*, **98** (1938), 31.

(13) Glauconite. Mean value of the chemical compositions of glauconite collected by "Challenger". W. H. Twenhofel, "Principles of Sedimentation", 1939, 401.

(14) Mean value of 12 analyses of glauconite reported by A. F. Hallimond, *Mineralog. Mag.*, **19** (1922), 330.

(15) Celadonite W. E. Maegdefrau and U. Hofmann, *Z. Krist.*, **98** (1938), 31.

(16) Celadonite. A. Lacroix, *Bull. soc. franç. minéral.*, **39** (1916), 93.

(17) Mean value of celadonite from Scotland. W. H. Twenhofel, "Principles of Sedimentation", 1939, 401.

(18) Mean value of the chemical analyses of celadonite reported by F. Heddle and L. L. Fermor, *Rec. Geol. Survey, India*, **58** (1926), 141, 330.

(19) "Grünerde". K. Hummel, *Chem. Erde*, **6** (1931), 468.

of glauconite and celadonite are not clearly shown. The writer showed the differnce as follows. From the accurate chemical compositions (Table 3) of glauconite and celadonite[11], the writer calcurated the values of R_2O_3 ($Al_2O_3+Fe_2O_3$) and RO($FeO+MgO$) as SiO_2: 2.00 and plotted them on Fig. 2. (c). From this figure, it is clearly shown that R_2O_3/RO is less than 1 in celadonite, while, the ratio is larger than 1 in glauconite.

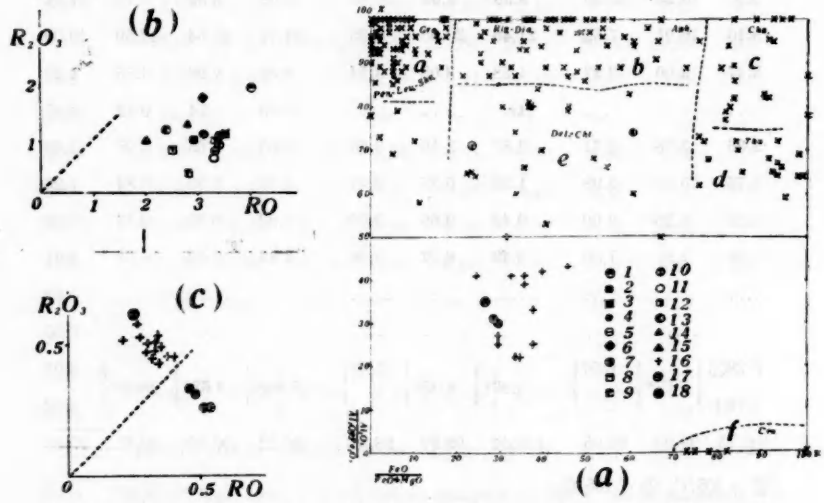

Fig. 2. Diagramatic expression of the chemical compositions of chlorites, glauconite, celadonite and "Grünerde". × : chlorites.

(a) Pen.-Leu.-She.-Gro. area: Penninite, Leuchtenbergite, Sheridanite, Grochauite, etc.
(b) Rip.-Dia.-Aph. area: Ripidolite, Diabantite, Aphrosiderite, etc.
(c) Cha. area: Chamosite.
(d) Thu. area: Thuringite.
(e) Del. area: Delessite, Chloropite, (Cinochlore, Prochlorite), etc.
(f) Cro. area: Cronstedite.

1, Amesite; 2, Aphrosiderite; 3, Bavalite; 4, Chamosite; 5, Clinochlore; 6, Cronstedite; 7, Daphnite; 8, Delessite; 9, Diabantite; 10, Leuchtenbergite; 11, Penninite; 12, Ripidolite; 13, Sheridanite; 14, Strigovite; 15, Thuringite; 16, Glauconite; 17, Celadonite; 18; "Grünerde" (by K. Hummel).

4. General expression of the chemical composition of chlorites.

About the chemical compositions of chlorites, the excellent generali-

(11) T. Yagi, *J. Japan. Assoc. Mineral. Petrol.Econ. Geol.*, **3** (1930), 119 (n Japanese); J. W. Gruner, *Am. Mineral.*, **20** (1935), 699; W. H. Twenhofel, "Principles of Sedimentation," 1939, 401; H. Schneider, *J. Geol.*, **35** (1927), 296; A. F. Hallimond, *Mineralog. Mag.*, **19** (1922), 330; **13** (1298), 68; K. Hummel, *Chem. Erde*, **6** (1931), 468; E. Maedgefrau and U. Hofmann, *Z. Krist.*, **98** (1938), 31; L. L. Fermor, *Rec. Geol. Survey, India*, **58** (1926), 141, 330; A. Lacroix, *Bull. soc. franç. minéral.*, **39** (1916), 93.

zation was reported by J. Orcel[12]. The crystal-structural formula of chlorite has been discussed recently by H. Berman[13] to be as follows.

$$(Mg, Fe'', Fe''', Al)_n(Al, Fe''', Si)_4O_{10}(OH)_{2(n-2)} \cdot s.\ H_2O$$

Namely the half of (Al, Fe''') replaces a part of Si and the other half of (Al, Fe''') replaces a part of (Mg, Fe'') and it was shown that the various ratios of RO/R_2O_3, Al_2O_3/R_2O_3, and FeO/RO produce many species of chlorite well known. The writer tried a general expression of the chemical compositions of chlorites by above three ratios. First the chemical compositions of chlorite are expressed by the ratio of R_2O_3/RO (where SiO : 200) in Fig. 2, (b). It is clearly shown from Fig. 2, (b) that the ratio of R_2O_3/RO is less than 1 in chlorites. Next the chemical compositions of the main chlorites are plotted in the diagram by the ratio of Al_2O_3/R_2O_3 and the ratio of FeO/RO as shown in the Fig. 2, (a). It is clearly shown, from Fig. 2, (a) that all the chemical compositions of chlorites are plotted in the area of $Al_2O_3/R_2O_3 \geqq 50$ % (except cronstedite), and the chlorite area may be divided into as follows.

(a) Mg-Al chlorite area...penninite, leuchtenbergite, sheridanite, grochauite, etc.

(b) Al-Fe''-Mg chlorite area...ripidolite, diabantite, aphrosiderite, etc.

(c) Fe''-Al chlorite area...chamosite.

(d) Fe'''-Al-Fe'' chlorite area...thuringite.

(e) Fe'''-Fe''-Al-Mg chlorite area...delessite, chlororite, clinochlore, prochlorite, etc.

(f) Fe'''-Fe'' chlorite area...cronstedtite.

For the sake of comparison, the chemical compositions of glauconite and celadonite are plotted in the Fig. 2, (a). As well shown from Fig. 2, (a), the plotted points of the chemical compositions of glauconite and celadonite ordinarily fall in the area of $Al_2O_3/Fe_2O_3 \leqq 50$ %.

Conclusion.

The writer tried a generalization of the chemical compositions of fine micas (including glauconite and celadonite) and chlorites and also tried a general expression of these chemical analyses to show some chemical characteristics of these minerals.

Geological Institute, Faculty of Science,
Tokyo University.

(12) J. Orcel, *Bull. soc. franç. minéral.*, **50** (1927), 75.
(13) H. Berman, *Am. Mineral.*, **22** (1937), 378.

On the Equilibrium of the Radioactive Elements in the Hydrosphere. III. On the Ratio of Thorium Emanation to Radium Emanation in the Hydrosphere.

By Kazuo KURODA and Yuji YOKOYAMA.

(Received Aug. 31, 1948.)

Introduction.

In the previous paper[1], the occurrence of thorium emanation in the mineral waters of Masutomi was reported by the present authors.

The ratio of thorium emanation to radium emanation in the spring B7 expressed in Mache unit was unexpectedly high and showed the values larger than 10. The authors tried to verify this quite unexpected fact by different methods. The radioactivity of the mineral waters of Masutomi and other famous radioactive springs of Japan was measured and it was found that thorium emanation occurs in many natural waters. The occurrence of thorium emanation was detected and its ratio to radium emanation was determined by the following methods, namely...(1) with the I. M. fontactoscope, (2) with the Lauritsen-type K. Y. fontactoscope, and (3) by the indirect method, in which the radioactivity of the decay products deposited on the negatively charged metals was measured.

I. The Radioactivity Measurements with the I. M. Fontactoscope.

It is not so difficult to obtain the decay curves due to thorium emanation with the I. M. fontactoscope, when the sample water contains considerably high amounts of thorium emanation. However, some technical skill is required, as the half period of thorium emanation is very short, and it disappears if we do not begin the measurements quickly.

The stagnant waters do not contain thorium emanation, and the mineral waters containing large amounts of thorium emanation issue vigorously from the orifice, in most cases directly from the gap in rocks. The samples must be taken very quickly with the injectors of the suitable size, and ejected vigorously in the ionization box of the I. M. fontactoscope. The radioactivity measurement is started as soon as possible. The examples of the decay curves are shown in Fig. 1. a. and Fig. 2. The ratio of the radioactivity of thorium emanation and radium emanation at the time when the sample was taken, is obtained by the extrapolation of the decay curves, as is shown in Fig. 3. Fig. 1. b. shows an example of decay curve of thorium X.

(1) K. Kuroda and Y. Yokoyama, this Bulletin, **21** (1948), 52, 58.

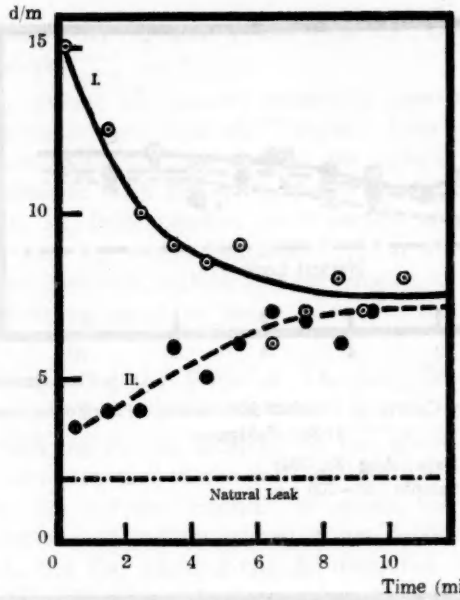

Fig. 1. (a) Decay Curve of Thorium Emanation (I. M. Fontactoscope) O-T-R, Misasa.

Date Aug. 27, 1948, 15h 13′ 30″
Sample; 100 c.c.

I. Radioactivity measurement started as soon as possible.
II. Radioactivity measurement started 5 minutes after the sample was taken with the injector. The decay curve of thorium emanation is not observed.

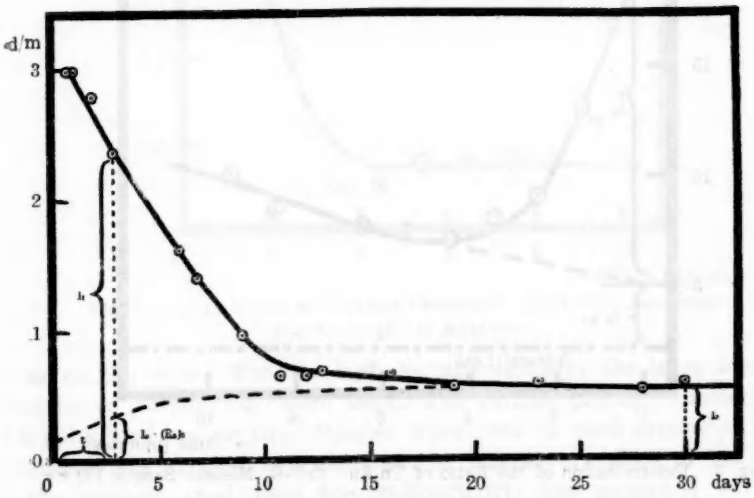

Fig. 1. (b) Determination of the ThX Content and the Ra Content. Masutomi Spring B7.

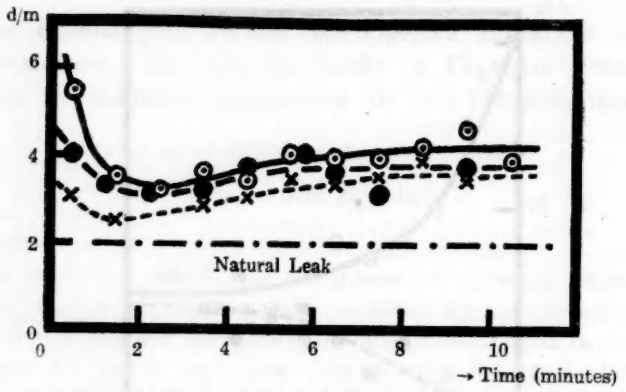

Fig. 2. Decay Curves of Thorium Emanation (I. M. Fontactoscope). O-K-1, Sekigane.

Date: Aug. 28, 1948
Sample: 50~100 c.c.

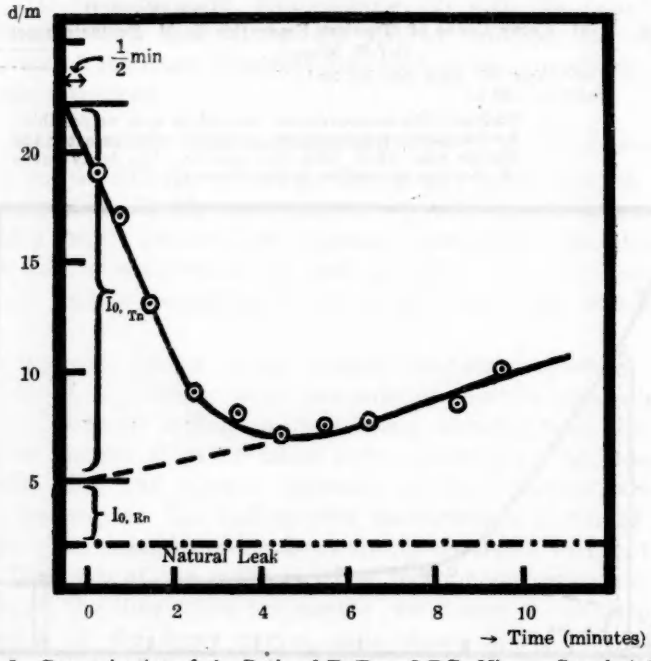

Fig. 3. Determination of the Ratio of Tn/Rn. O-T-R, Misasa. Sample 100 c.c.

II. The Radioactivity Measurements with the Lauritsen-type K. Y.-Fontactoscope.

The decay curves of thorium emanation was also obtained by the radioactivity measurement with the Lauritsen-type K. Y. fontactoscope.

It was rather difficult to determine the ratio of thorium emanation to radium emanation with the K. Y. fontactoscope, compared with the case of the I. M. fontactoscope, as it needed more time to take the sample water into the radon container and to start the radioactivity measurements. However, satisfactory agreements were obtained by these methods. The examples of the decay curves of thorium emanation are shown in Fig. 4.

III. Determination of the Ratio of Thorium Emanation to Radium Emanation by the Indirect Method.

To ascertain the results obtained by the above-mentioned methods, we tried the determination of the ratio of thorium emanation to radium emanation by the indirect method, in which the decay products of thorium emanation and radium emanation are deposited on the negatively charged wires, and the radioactivity is measured with tne Lauritsen-electroscope. Fig. 5 shows the apparatus to collect the decay pro-

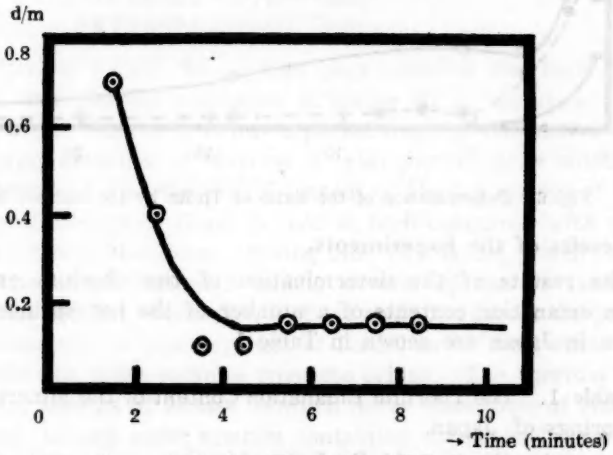

Fig. 4. Decay Curve of Thorium Emanation. (K.Y. Fontactoscope) The Spring B7 in Masutomi.

ducts on the wire. For the high voltage battery, the layer built dry batteries of Toshiba Co. were used. The voltage of single battery was 67.5 volts, and one or two batteries were used in each apparatus. This apparatus was exposed overnight at the places very close to the orifice of the springs, and then the radioactivity was measured with the Lauritsen-electroscope.

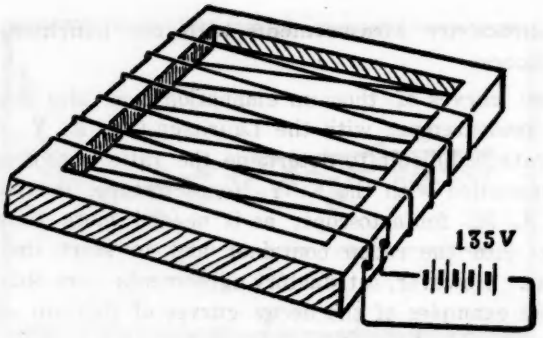

Fig. 5. Apparatus used for collecting the Decay Products of Thorium Emanation and Radium Emanation.

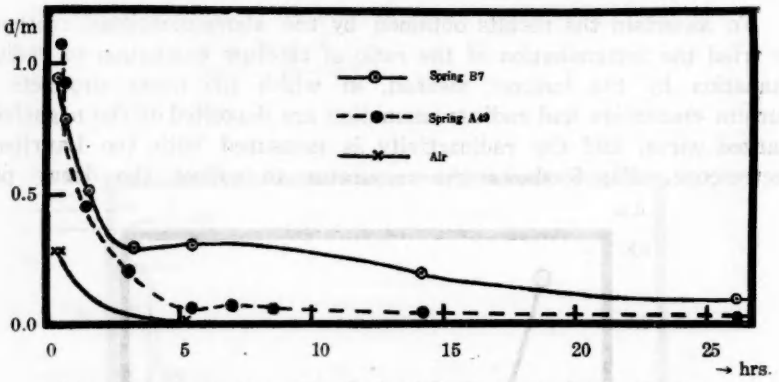

Fig. 6. Determination of the Ratio of Tn/Rn by the Indirect Method.

IV. Results of the Experiments.

The results of the determination of the thorium emanation and radium emanation contents of a number of the hot springs and mineral springs in Japan are shown in Table 1.

Table 1. The Thorium Emanation Content of the Mineral Springs and Hot Springs of Japan.

Masutomi. (Yamanashi Prefecture)

Name	Thorium Emanation Content (Mache)	Radium Emanation Content (Mache)	Apparatus
B7	95	6.27	
A3	15	2.2	
A3′	15	5.9	I.M.
A3″	10	—	
A1	10	—	
A49	absent	about 5000	
Gas from the spring B7	107	19.5	

Ikeda. (Simane Prefecture)

No. 1	absent		K.Y.
No. 3	330	130	

Misasa. (Tottori Prefecture)

O-T-R (Ōhasi-Ryokan)	450	80	I.M.
Matubara	8	26	

Sekigane. (Tottori Prefecture)

O-K-1 (Onseirō-Ryokan)	100	30	I.M.
O-K-2	30	30	
O-U	30	30	
O-N-C	30	30	

Arima. (Hyogo Prefecture)

Tansan-Onsen (Small spring)	20-40	ca. 5	I.M.
Sakae-Kōsen	10	ca. 5	

Remark: The thorium emanation content was expressed in Mache unit. It is defined as follows: it is called 1 Thoron-Mache when 0.001 e.s.u. of saturation current is obtained by thorium emanation and its equilibrium amount of thorium A in 1 litre of the sample water.

$$1\,\text{Tn Mache} = 1.52\times10^{-10}\ \text{Curie/l.}$$
$$1\,\text{g Th unit} = 1.11\times10^{-7}\ \text{Curie.}$$

In the previous paper, the authors have reported the high content of thorium X and thorium emanation in spring B7 in Masutomi. From the experiments in Masutomi, it was expected that the radioactive springs containing large amounts of thorium X, also contain large amounts of thorium emanation. The thorium X content of the hot springs of Misasa and the mineral springs of Ikeda is not so high compared with that of the mineral springs of Masutomi. Spring No. 3 in Ikeda, which contains the highest amount of thorium X among several springs in Ikeda, was found to contain thorium emanation, but we could not detect the presence of thorium emanation in other springs of Ikeda, as in most cases it was difficult to take the fresh samples from the orifice. The thorium X content of the hot springs of Misasa is much lower than those of Masutomi and Ikeda, and though eight samples containing considerably large amounts of thorium X were measured, thorium emanation was not detected excepting one sample. This was Matubara-no-yu (yu = spring), in which 2.1×10^{-5} g of thorium was found in 1 litre, by Mr. K. Shimokata. The Ōhasi-Ryokan-Soto-Yu showed the highest content of thorium X among the springs of Misasa, but thorium emanation was not detected. Therefore, we concluded that the hot springs of Misasa do not contain the high amounts of thorium emanation, when we visited there for the first time in May of 1948. However, in August of 1948, the radioactivity was

measured with the special-sized counter, and it was found that some springs in Misasa show unexpectedly high radioactivity, whereas their radon or radium contents are not unusual. For example, a spring in the hotel "Ōhasi", called "Tennen-Gankutu-no-yu-Reisen" (O-T-R), showed unexpectedly strong radioactivity when it was examined with the counter. This spring was carefully examined repeatedly with the I. M. fontactoscope, and it was found that the fresh sample of this spring shows high content of thorium emanation. The thorium emanation content of this spring is the highest ever observed in this country and probably in the world.

The hot springs of Sekigane, and the hot springs of Arima were also studied in the summer of 1948, and it was found that the springs containing not so high amounts of thorium X, sometimes contain the considerable amounts of thorium emanation. The authors consider that most radioactive springs contain thorium emanation, but it was not detected by the previous investigators, as the samples were taken from the stagnant springs and as the radioactivity measurements were started very deliberately. The distribution of thorium emanation accompanied by radium emanation in many mineral waters shows that the source of these elements is not so deep under the ground.

The determination of the ratio of thoron to radon by the indirect method was carried out in the summer of 1948, in Masutomi and in Arima. The experimental results are shown in Table 2.

Table 2. The Determination of the Ratio of Thoron to Radon by the Indirect Method.

	Spring B7			Spring A49			In the Air (At the hotel Tuganero)		
Length of the Wire	2 m.			1 m.			2 m.		
Voltage	135 volts			67.5 volts			135 volts		
Beginning of Exposure	19h 10, July 2			19h 00, July 2			19h 00, July 3		
End of Exposure	7h 04, July 3			7h 06, July 3			9h 16, July 4		
Exposed Time	11 hrs 54 m			12 hrs 06 m			14 hrs 16 m		
	t	$I_{obs.}$	$I_{cal.}$	t	$I_{obs.}$	$I_{cal.}$	t	$I_{obs.}$	$I_{cal.}$
	m	d/m		m	d/m		m	d/m	
	26	0.94	0.90	30	1.08	1.06	22	0.27	0.28
	40	0.78	0.82	40	0.92	0.94	27	0.27	0.26
	1h 35	0.52	0.59	1h 26	0.46	0.45	5h 17	0.00	0.00
	3h 20	0.39	0.43	3h 09	0.21	0.12			
	5h 23	0.40	0,38	5h 22	0.06	0.08			
	14h 14	0.19	0.21	6h 59	0.08	0.07			
	27h 33	0.10	0.09	8h 37	0.07	0.06			
	50h 11	0.04	0.02	14h 11	0.04	0.04			
				27h 39	0.01	0.02			
I_0ThB, C	0.49 d/m			0.10 d/m			0.00 d/m		
I_0RaB, C	0.48 ,,			1.18 ,,			0.31 ,,		
I_∞ThB, C	0.99 ,,			0.20 ,,			0.00 ,,		
Thoron/Radon (Curie/Curie)	2.06			0.17			0·00		

In Table 2. I_0 *ThB,C* (= ionization current of thorium B and thorium C at t = 0, when the exposure finished) is calculated from the values of ionization current after RaB and RaC have completely disintegrated. The values of ionization current due to ThB and ThC at each time were calculated and these values were subtracted from the observed values of ionization current (I_{OBS}). The values of ionization current due to Ra B and Ra C are obtained here, and from these values, I_0 *RaB, C* (Ionization current due to RaB and RaC at (t = 0) is obtained.

Now, the amount of thorium C formed from thorium emanation in 12 hours is 49.6 % of the equilibrium value, the values of ionization current due to thorium B, C when the activation reached the saturation value (I_∞*ThB, C*) are then calculated. The ratio of Tn/Rn is obtained from the ratio of I_∞*ThB, C*/I_0 *RaB, C*. $I_{cal.}$ is the calculated value from the values of I_0 *RaB, C* and I_0*ThB, C*. The decay curves and theoretical values showed satisfactory agreements. However, the ratio of Tn/Rn in the atmosphere above the orifice of the springs is obtained by this method, and this value will be different from the ratio of Tn/Rn in the mineral springs. The thorium emanation and radium emanation content of the spring B7 expressed in Curie unit is as follows.

$$\text{Tn} = 144 \times 10^{-10} \text{ Curie/l.}$$

$$\text{Rn} = 20 \times 10^{-10} \text{ Curie/l.}$$

Therefore, the ratio of Tn/Rn in the spring B7 is about 7 expressed in Curie unit. The ratio in the atmosphere on the orifice of the spring B7 is considerably lower than this value, as is shown in Table 2. The reason for this is probably because the half period of thorium emanation is very short and it disintegrates as soon as it issued from the orifice.

The thorium emanation content of the spring A49 was not determined by the direct methods. However it is estimated from the result of indirect determination to be as follows, if we assume that the conditions are same in both spirngs (B7 and A49).

Rn content of the spring A49 = about 17000×10^{-10} Curie/l.

Tn/Rn in the atmosphere near A49 = 0.17

As the ratio [(Tn/Rn) in the air]/[(Tn/Rn) in the water] was 2/7 in the case of the spring B7, the ratio Tn/Rn in the spring water of A49 will be about 0.6.

Therefore, the Tn content of the spring A49

$$= \text{about } 10000 \times 10^{-10} \text{ Curie/l.}$$

$$= \text{about } 6600 \text{ Tn-Mache.}$$

(Remark ; 1 thoron-Mache = 1.52×10^{-10} Curie/l.)

The determination of the ratio of Tn/Rn was also tried at Arima. In the atmosphere near the orifice of Tansan-Onsen, the decay products o-

thorium emanation were detected, but their radioactivity was very weak, and the radioactivity due to the decay products of radium emanation was not detected.

Table 3. The Determination of the Ratio of Thoron to Radon by the Indirect Method. "Tansan-Onsen" at Arima, Hyōgo Prefecture.

Exposure		19h 40, Sept. 2, ...7h 40, Sept. 3			
Voltage		−135 V			
T (m)	40	1h 42 m	2h 46 m	5h 16 m	10h 0 m
I (d/m)	0.06	0.07	0.07	0.07	0.045

From this, the ratio of Tn/Rn in the atmosphere near the orifice of the "Tansan-Onsen" is considered to be about 10 or larger. Therefore, the ratio of Tn/Rn in the atmosphere at Tansan-Onsen is considerably larger than that of the spring water.

This result is quite different from the result obtained in Masutomi, and further investigation is necessary.

Summary.

The ratio of thorium emanation to radium emanation in natural waters was measured. Following three methods were used: (1) with the I. M. fontactoscope, (2) with the Lauritsen-type K. Y. fontactoscope, and (3) the indirect method, in which the radioactivity of the decay products of thorium emanation and radium emanation is measured with the Lauritsen-electroscope.

It was found that thorium emanation is considerably widely distributed in the mineral springs and hot springs of Japan.

The authors take this opportunity of heartily thanking Prof. Kenjiro Kimura for his kind guidance in the course of this study. The cost of this research was defrayed from the Scientific Research Encouragement Grant from the Ministry of Education, to which our thanks are due.

Chemical Institute, Faculty of Science,
Tokyo University.

On the Equilibrium of the Radioactive Elements in the Hydrosphere. IV. On the Ratio of Thorium X to Radium in the Hydrosphere.

by Kazuo KURODA and Yuji YOKOYAMA.

(Received Aug. 31, 1948.)

Introduction.

In the previous paper[1], the occurrence of thorium X in the mineral waters of Masutomi was reported by the authors. The ratio of thorium X to radium expressed in Curie unit was considerably large in the case of Masutomi. The highest value of this ratio was 10.3 of the spring B7. This ratio was larger than 1 in many springs in Masutomi, and it was considerably larger than the value obtained by Kurbatov in three springs of Gelesnovdsk (0.02 to 0.58). Is this ratio also large in other radioactive springs of Japan or not? The authors have intended to determine the ratio of thorium X to radium in the mineral springs of Ikeda and in the hot springs of Misasa.

I. Determination of Thorium X and Radium.

Radium and thorium X were co-precipitated together with barium sulphate from 1 to 3 litres of the mineral water, and the radioactivity of the powdered precipitate was measured with the Lauritsen-electroscope. The radioactivity diminishes slowly for several days, according to the presence of thorium X. The radioactivity becomes constant after about thirty days and this radioactivity is due to radium. The thorium X content ($C\ ThX$) and the radium content ($C\ Ra$) were obtained from the equations

$$CRa = I_e K_{Ra} \qquad (1)$$

and

$$CThX = \frac{I_t - I_e(Ra)_t}{(ThX)_t} \times K_{ThX} \qquad (2)$$

where, I_t = observed radioactivity at time t,
I_e = observed radioactivity at $t = 30$ days,
$(Ra)_t$ = the factor of the radioactivity of radium to calculate the radioactivity at each time,
$(ThX)_t$ = the degree of the disintegration of thorium X in time t,
K_{ThX} and K_{Ra} = sensitivity of the instrument for thorium X or radium, and their values were as follows:

(1) K. Kuroda and Y. Yokoyama, this Bulletin, **21** (1948), 52.

$$K_{Ra} = 83 \times 10^{-12} \text{ g per div. per min.} \quad (3)$$

and $$K_{ThX} = 75 \times 10^{-12} \text{ Curie per div. per min.} \quad (4)$$

II. Results.

The results obtained are shown in Table 1 and Table 2. The thorium X contents are shown in two units, their relation being as follows.

$$\text{g Th/l} = 1.11 \times 10^{-7} \text{ Curie/l.} \quad (5)$$

Table 1. The Thorium X and Radium Content of the Hot Springs of Misasa. (May 5, 1948).

Name	Temp. °C	Rn 10^{-10}C/l	I_t	I_c	Ra 10^{-12}g/l	ThX 10^{-12}C/l	ThX 10^{-5}gTh/l
(1) Okayama Univ.	61	40	0.31	0.14	12	23	21
(2) Misasa Hotel	58	18	0.36	0.22	18	26	23
(3) Ohasi-Soto-Yu	49	38	1.03	0.14	12	80	72
(4) Matubara	61	70	0.34	0.23	19	25	23
(5) Tennen-Gankutu	43	260	0.28	0.10	8	21	19
(6) Tabakoya	38	560	0.30	0.04	3	24	22
(7) Yamadaku	55	900	0.03	0.03	3	2	2
(8) Hanaya	59	650	0.03	0.03	3	2	2
(9) Akasakiya	42	180	0.02	0.05	4	0.5	0.5

Table 2. The Thorium X and the Radium Content of the Mineral Springs of Ikeda.

Name	Temp. °C	Rn 10^{-10}C/l	I_t	I_c	Ra 10^{-12}g/l	ThX 10^{-12}C/l	ThX 10^{-5}gTh/l
No.1	15	480	1.35	0.50	41	108	97
No.2	16.5	380	1.24	0.53	44	98	88
No.3	16	770	1.37	0.50	42	111	100
No.4	13	6100	0.18	0.29	24	9	8
No.5	12.5	8500	0.06	0.07	6	4	4
Oku-no-yu	22	(20)	0.64	0.25	21	50	45

Table 1 and Table 2 show that the ratio of thorium X to radium is also large in the mineral springs of Ikeda and the hot springs of Misasa. The highest value was 8.0 in the spring water of Akasakiya in Misasa. The following rules were found in Ikeda and in Misasa, namely: (1) the higher the water temperature and the larger the amount of flow, the larger is the ratio of ThX/Ra, and (2) the larger the radium content and the smaller the radon content, the larger is the thorium X content. These tendencies are quite similar to those obtained in Masutomi, but they are not so clear compared with the case of Masutomi. It is probably because the springs issue from the bottom of the bath, and we sometimes used stagnant waters. The ratio of thorium X to radium in these mineral springs are summarized in Table 3 and Table 4.

Table 3. The ThX/Ra Ratio in 25 springs of Masutomi.

ThX/Ra	<1	1-2	2-4	4-6	>6
Number of springs	7	4	5	5	2

Table 4. The ThX/Ra Ratio in 15 Springs of Misasa and Ikeda.

ThX/Ra	<1	1-2	2-4	4-6	>6
Number of springs in					
Misasa	3	3	1	0	2
Ikeda	2	0	4	0	0

Summary.

The thorium X and radium contents of mineral springs of Ikeda and the hot springs of Misasa were estimated. The ratio of thorium X to radium in these springs was considerably larger than that obtained by Kurbatov in Gelesnovdsk. The relation between the ratio of thorium X and radium, and water temperature, radium content, radon content, etc., was quite similar to that found in Masutomi.

The authors take this opportunity of heartily thanking Prof. Kenjiro Kimura for his kind guidance in the course of this study.

The cost of this research was defrayed from the Scientific Research Encouragement Grant from the Ministry of Education, to which our thanks are due.

Chemical Institute, Faculty of Science,
Tokyo University.